65 p.

N64-18489

Code 1

NASA CR-52427

[redacted]

A BLAST-WAVE THEORY OF CRATER FORMATION IN SEMI-INFINITE TARGETS[*]

by

William J. Rae[**] and Henry P. Kirchner[***]

Cornell Aeronautical Laboratory, Inc.
Buffalo 21, New York

[*]This research was sponsored by the National Aeronautics and Space Administration under Contract No. NAS 3-2121

[**]Research Aerodynamicist, Aerodynamic Research Department

[***]Staff Scientist, Computer Research Department

BLAST-WAVE THEORY OF CRATER FORMATION

ABSTRACT

An analytic formulation of the problem of crater formation is presented, using the methods of blast-wave theory. The approximations on which this approach is based are chiefly concerned with the self-similar, or progressing-wave nature of the solution, with the type of state equation used, and with the extent to which the conservation of energy and momentum can be fulfilled. These approximations and the limitations which they impose are reviewed, particularly as applied to the problem of shock propagation in solids. Neglect of momentum conservation is shown to be a good approximation, but use of the Mie-Grüneisen equation of state is found to be largely incompatible with the assumption of similarity. An approximate nonsimilar solution for impact-generated shock propagation is derived, and displays excellent agreement with observed shock-wave trajectories.

To derive a penetration law from any solution, some point in the trajectory must be chosen as the crater radius. The strong influence of this choice on the penetration law is discussed, and it is argued that the target strength should play a role in its determination. A simple choice of the crater-formation criterion, related to the intrinsic shear strength of the target, is utilized in conjunction with the nonsimilar solution, to derive a penetration law which correlates a large amount of data.

BLAST-WAVE THEORY OF CRATER FORMATION

TABLE OF CONTENTS

ABSTRACT		164
INTRODUCTION		166
1.	Basic Equations	170
2.	Similarity Assumption and its Implications	175
3.	The Equation of State	179
4.	Conservation of Energy and Momentum	182
5.	Taylor Solution for Shock Propagation	197
6.	Quasi-Steady Solution for Shock Propagation	201
7.	Methods of Crater-Size Prediction	209
CONCLUDING REMARKS		215
REFERENCES		217
APPENDIX: Simulation of Meteoroid Impact by Energy Release		220
ACKNOWLEDGEMENT		225
LIST OF SYMBOLS		226

BLAST-WAVE THEORY OF CRATER FORMATION

INTRODUCTION

The fluid-mechanical approximation pioneered by Bjork[1] is commonly accepted as a proper description of the early phases of target deformation due to hypervelocity impact. In such a model, the motion of any small mass element is assumed to be governed by the pressures acting on its faces, while resistance to shear deformation is neglected. The differential equations that govern such inviscid motion are the usual Euler equations expressing the conservation of mass, momentum, and energy, together with the equation of state of the compressible medium. These differential equations contain two spatial variables, as well as the time, and the problem of solving them is extremely difficult. To date, the only solutions that have been reported are the numerical results of Bjork.[1,2]

The purpose of this paper is to present an approximate analytic solution of the same set of equations. The solution is achieved by adapting the techniques of blast-wave theory, which has produced such rich dividends in the study of various high-energy fluid-flow problems.[3,4,5] The spirit of the approach is to simplify the analysis wherever possible by making certain approximations to the true physical situation. We seek generality and simplicity in the results. Some exactness in specifying details of the problem must, of course, be sacrificed.

The blast-wave theory has been developed, over the years, as a means of describing various high-energy gas flows. In order to apply such a theory to the problem of cratering by high-speed projectiles, each of its approximations must be carefully examined in this new context.

The most important approximations can be grouped into three main categories; first, those concerned with the assumption of a self-similar form of solution, second, those associated with the equation of state of the medium, and third, those dealing with the extent to which global energy- and momentum-conservation conditions can be satisfied. After a brief review of the basic fluid-mechanical equations in Section 1, these three categories are discussed in detail in Sections 2, 3, and 4. Following this, Sections 5 and 6 present two different approximate solutions for the time-history of the shock as it penetrates the target. Finally, Section 7 takes up the question of crater-size prediction.

The assumption of similarity discussed in Section 2 supposes that the flow pattern behind the shock that advances into the target is always the same, if viewed on a scale given by the depth to which the shock has penetrated at that instant. This approximation has the effect of suppressing time as an independent variable, and constitutes a key mathematical simplification. At the same time, it imposes certain restrictions, the most important of which is that only certain forms of the state equation are permitted. Section 3 discusses the extent to which the Mie-Gruneisen equation approximates the permitted form. It is found that only the extremely high-pressure states of a Mie-Grüneisen material fulfill the required form, and in that range, the true equation of state can be replaced by a perfect gas of constant specific-heat ratio. In every impact, the shock ultimately degenerates to a stress wave, so that the high pressures required for the perfect-gas approximation are only achieved during a small portion of the process. Thus, a realistic description of shock propagation in solids requires a solution which accounts for the nonsimilar nature of the problem.

BLAST-WAVE THEORY OF CRATER FORMATION

To conserve the total energy and momentum of the impacting particle, the solution must allow for spatial variations in two dimensions, and consequently a set of partial differential equations must be solved. Section 4 describes approximate solutions of these equations along the axis of symmetry, and compares these results with those obtained using only one spatial variable, the distance from the impact point. Solutions with only one spatial coordinate can conserve only the total energy of the system, and are found to be practically identical with the more complicated two-dimensional solutions. A corollary of this finding is that the energy of the projectile is the more important parameter, its momentum playing only a secondary role. In Section 4, the physical reasons for this behavior are described, and its implications on simulation of hypervelocity impact are discussed.

Sections 5 and 6 are devoted to a description of the trajectory traced out by the shock as it propagates through the target. The classical Taylor solution for self-similar motion of a shock through a perfect gas is reviewed in Section 5. With this as a background, we then present in Section 6 an approximate solution which allows for the nonsimilar nature of shock propagation in solids. In this solution, the shock speed tends naturally to the stress-wave limit at large time. Comparisons with experimental observations in transparent targets, and with Bjork's calculated shock trajectories, reveal an excellent correlation over a wide range of conditions. This correlation uses only the energy of the projectile, and the density and stress-wave velocity of the target. The fact that data up to an impact speed of 30 Km/sec are all correlated suggests that impact-generated shock propagation follows essentially the same mechanism over the entire speed range.

BLAST-WAVE THEORY OF CRATER FORMATION

To predict crater size, the solution for shock position as a function of time is not enough. Section 7 points out that an auxiliary criterion is needed, to identify the point at which the crater will form. The correlation presented here indicates that the choice of this criterion is the most important factor in determining the ultimate penetration law. In Section 7, the question of choosing a proper crater-formation criterion is not settled, but several choices are discussed. One of these is shown to be capable of correlating a large amount of data, thro' gh proper selection of a certain constant.

The net effect of these studies has been to reveal the potentialities and the limitations of blast wave theory, as applied to crater formation in semi-infinite targets. Considerable progress has been made, notably in establishing the relative unimportance of momentum conservation, and in identifying the nonsimilar nature of the problem, and its connection with the Mie-Grüneisen state equation. At the same time, a great deal of work remains to be done in certain othe areas, especially in regard to the formulation of a suitable criterion for crater formation.

BLAST-WAVE THEORY OF CRATER FORMATION

1. BASIC EQUATIONS

When a particle strikes a target surface at high speed, large amounts of energy and momentum are quickly transferred to a very small portion of the surface. Consequently, a strong shock wave is driven into the target, generating extremely large pressures, typically measured in megabars. Because these pressures are so large compared with the material strength, one is led to the approximation that the impacted medium behaves like an inviscid, compressible fluid. In fact, the justification for such an approximation is not provided by the magnitude of the pressure themselves, but must come from a consideration of their gradients. Consider a small mass element

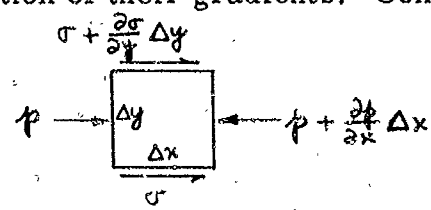

The net force acting in the x-direction is proportional to $\frac{\partial \sigma}{\partial y} - \frac{\partial p}{\partial x}$; thus the neglect of resistance to shear deformation requires $\frac{\partial p}{\partial x} \gg \frac{\partial \sigma}{\partial y}$. To replace this comparison of gradients by a simple comparison of pressure with strength, is to assume that rates of change in the two perpendicular directions are of the same order, and that the proper orders of magnitude to use for p and σ are the impact pressure and material strength at high strain rates. There appears to be no reason for doubting either of these assumptions in the early stages of the impact process. Thus the problem of determining the response of the target material becomes essentially that of solving the fluid-mechanical equations (conservation of mass, momentum and energy) together with the equation state of the medium

Mass: (1)

$$\frac{D\rho}{Dt} + \rho \, \mathrm{div} \, \vec{q} = 0$$

Momentum: (2)

$$\rho \frac{D\vec{q}}{Dt} + \mathrm{grad} \, p = 0$$

Energy: (3)

$$\frac{De}{Dt} + p \frac{D(1/\rho)}{Dt} = 0 \quad \text{or} \quad \frac{Ds}{Dt} = 0$$

Equation of State: (4)

$$e = F(p, \rho)$$

Here, ρ denotes the density, p the pressure, e the internal energy per unit mass, s the entropy per unit mass, and $\vec{q}$ the velocity vector. The symbol D/Dt is the convective derivative –

$$\frac{D}{Dt} = \frac{\partial}{\partial t} + \vec{q} \cdot \nabla \qquad (5)$$

in which t is the time and ∇ the gradient operator. It should be noted that the assumption of an inviscid fluid has been made by setting the right-hand side of Eq. (2) equal to zero. If shearing forces were to affect the motion, they would appear in this equation. Consistent with this approximation, energy changes arising from viscous dissipation and heat conduction are omitted from the energy equation. In addition, energy changes due to radiation and chemical change are neglected. Thus the conservation of energy simply states that for each element of mass, changes of internal energy de are balanced by changes in the flow-work term $p\,d\frac{1}{\rho}$. Alternatively, this condition may be expressed by stating that the entropy of a given mass element does not change after it has been processed by the shock.

Finally, it should be noted that the use of an equation of state implies the assumption of thermodynamic equilibrium.

It is assumed that the target motion is symmetric about an axis normal to the original target surface. For such an axisymmetric flow, the scalar forms of the equations of motion in spherical coordinates are

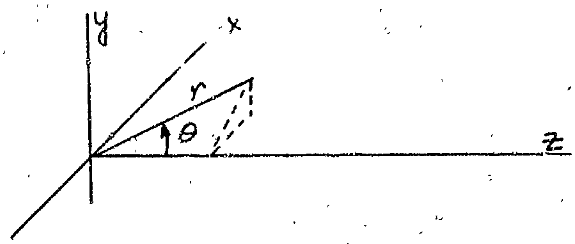

(x, y plane is the target surface)

$$\frac{\partial \rho}{\partial t} + u\frac{\partial \rho}{\partial r} + \frac{w}{r}\frac{\partial \rho}{\partial \theta} + \rho\left(\frac{\partial u}{\partial r} + \frac{1}{r}\frac{\partial w}{\partial \theta} + \frac{2u}{r} + \frac{w}{r}\cot\theta\right) = 0 \tag{6}$$

$$\frac{\partial u}{\partial t} + u\frac{\partial u}{\partial r} + \frac{w}{r}\frac{\partial u}{\partial \theta} - \frac{w^2}{r} + \frac{1}{\rho}\frac{\partial p}{\partial r} = 0 \tag{7}$$

$$\frac{\partial w}{\partial t} + u\frac{\partial w}{\partial r} + \frac{w}{r}\frac{\partial w}{\partial \theta} + \frac{uw}{r} + \frac{1}{\rho r}\frac{\partial p}{\partial \theta} = 0 \tag{8}$$

$$\frac{\partial e}{\partial t} + u\frac{\partial e}{\partial r} + \frac{w}{r}\frac{\partial e}{\partial \theta} - \frac{p}{\rho^2}\left(\frac{\partial \rho}{\partial t} + u\frac{\partial \rho}{\partial r} + \frac{w}{r}\frac{\partial \rho}{\partial \theta}\right) = 0 \tag{9}$$

$$e = F(p, \rho) \tag{10}$$

Here u and w denote the velocity components in the r- and θ- directions respectively. Equations (6) to (10) constitute five relations for the quantities p, ρ, u, w and e. One can also work with the entropy, rather than the internal energy, in which case the last two equations are replaced by

$$\frac{\partial s}{\partial t} + u\,\frac{\partial s}{\partial r} + \frac{w}{r}\,\frac{\partial s}{\partial \theta} = 0 \tag{11}$$

$$s = s(p, \rho) \tag{12}$$

The boundary conditions that apply at the shock wave, i.e. at $r = R_s(\theta, t)$, state that the discontinuities in velocity, pressure, density, etc. across the wave are given by the Rankine-Hugoniot relations. For a shock advancing into a medium at rest these are

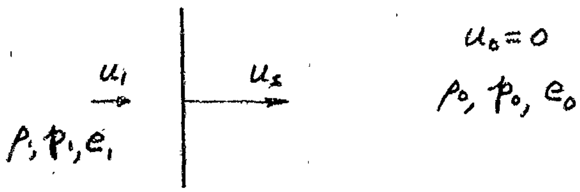

$$\rho_0 u_s = \rho_1 (u_s - u_1) \tag{13}$$

$$p_1 - p_0 = \rho_0 u_s u_1 \tag{14}$$

$$e_1 - e_0 = \frac{1}{2}(p_0 + p_1)\left(\frac{1}{\rho_0} - \frac{1}{\rho_1}\right) \tag{15}$$

In the analysis of this paper, it is assumed that the shock wave is always hemispherical in shape as it advances into the target. This assumption is based on observations of shock shape in lucite[6,7] and in wax[8,9] under hyper-velocity impact conditions. Further verification comes from the nearly hemispherical shape of the craters formed at high impact speed.

At this point, then, the fluid-mechanical problem posed is the solution of Eqs. (6) to (10), which describe the motion of an inviscid, compressible fluid, behind a hemispherical shock wave advancing into a semi-infinite target.

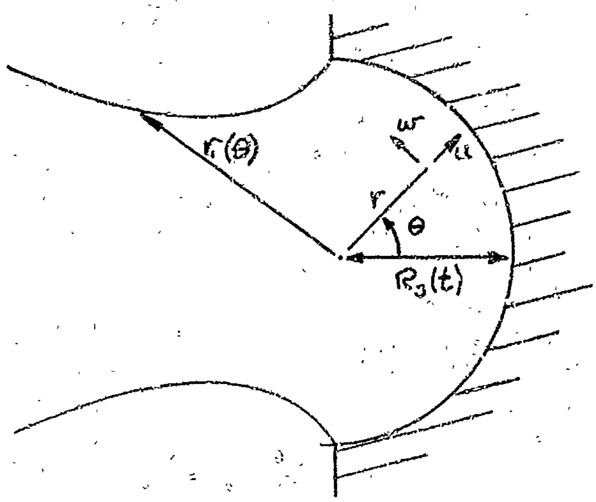

The motion must be such that the boundary conditions (13) to (15) are satisfied at the shock, while along the surface $r = r_1(\theta)$ (whose location is unknown) the pressure and material density must vanish.

The solution of such a boundary-value problem is an extremely difficult task. To date only numerical solutions have been presented.[1] The object of the present paper is to review the approximations of blast-wave theory and then to apply them in an effort to derive an analytic solution.

2. SIMILARITY ASSUMPTION AND ITS IMPLICATIONS

Mathematically speaking, the most important approximation made in the blast-wave theory is the assumption that the flow is self-similar, i.e. the distributions of the various physical quantities (such as pressure, density, etc.) at each instant are taken to be the same when viewed on a scale defined by the shock radius at that instant. Thus each quantity, instead of depending separately on the time and on the distance r from the impact point, is assumed to be a function only of the combination $r/R_s(t)$. This reduction of the number of independent variables constitutes a significant simplification in the differential equations that must be solved. The essence of the similarity assumption is to suppress time as an independent variable. This is done by introducing the similarity coordinate

$$\eta = \frac{r}{R_s(t)} \tag{16}$$

and by redefining the velocity components, pressure, density, and internal energy by the dimensionless functions

$$\begin{aligned} u(r,\theta,t) &= \dot{R}_s\,\phi(\eta,\theta) & p(r,\theta,t) &= \rho_0\dot{R}_s^2\,f(\eta,\theta) \\ w(r,\theta,t) &= \dot{R}_s\,\omega(\eta,\theta) & \rho(r,\theta,t) &= \rho_0\,\psi(\eta,\theta) \\ & & e(r,\theta,t) &= \dot{R}_s^2\,g(\eta,\theta) \end{aligned} \tag{17}$$

When these relations are substituted into Eqs. (6) to (9) and derivatives with respect to r and t are replaced in terms of derivatives with respect to η, one finds that all explicit time dependence can be suppressed from the differential equations if one chooses

$$R_s = At^N \tag{18}$$

Thus, out of the whole set of solutions of the basic equations, the similarity assumption restricts us to that subset for which the shock radius is proportional to a power of the time. When this is done the basic equations become

$$(\phi-\eta)\frac{\partial\psi}{\partial\eta}+\frac{\omega}{\eta}\frac{\partial\psi}{\partial\theta}+\psi\left(\frac{\partial\phi}{\partial\eta}+\frac{1}{\eta}\frac{\partial\omega}{\partial\theta}+2\frac{\phi}{\eta}+\frac{\omega}{\eta}\cot\theta\right)=0 \tag{19}$$

$$-\frac{1-N}{N}\phi+(\phi-\eta)\frac{\partial\phi}{\partial\eta}+\frac{\omega}{\eta}\frac{\partial\phi}{\partial\theta}-\frac{\omega^2}{\eta}+\frac{1}{\psi}\frac{\partial f}{\partial\eta}=0 \tag{20}$$

$$-\frac{1-N}{N}\omega+(\phi-\eta)\frac{\partial\omega}{\partial\eta}+\frac{\omega}{\eta}\frac{\partial\omega}{\partial\theta}+\frac{\phi\omega}{\eta}+\frac{1}{\eta\psi}\frac{\partial f}{\partial\theta}=0 \tag{21}$$

$$-2\frac{1-N}{N}g+(\phi-\eta)\frac{\partial g}{\partial\eta}+\frac{\omega}{\eta}\frac{\partial g}{\partial\theta}-\frac{f}{\psi^2}\left\{(\phi-\eta)\frac{\partial\psi}{\partial\eta}+\frac{\omega}{\eta}\frac{\partial\psi}{\partial\theta}\right\}=0 \tag{22}$$

The parameter N which appears here is for the moment unspecified.

After elimination of time as an explicit variable in the differential equations, the next step is to see if the boundary conditions are compatible with the similarity assumption. At the shock $\left(\eta=1,\ -\pi/2\leq\theta\leq+\pi/2\right)$ equations (13), (14), (15) and (10) become

$$\psi(1,\theta)\left[1-\phi(1,\theta)\right]=1 \tag{23}$$

$$f(1,\theta)=\phi(1,\theta)+\frac{p_0}{\rho_0\dot{R}_s^2} \tag{24}$$

$$g(1,\theta)=\frac{1}{2}\left[\frac{p_0}{\rho_0\dot{R}_s^2}+f(1,\theta)\right]\left[1-\frac{1}{\psi(1,\theta)}\right] \tag{25}$$

$$\dot{R}_s^2\,g(1,\theta)=F\left[\rho_0\dot{R}_s^2 f(1,\theta),\ \rho_0\psi(1,\theta)\right] \tag{26}$$

The first three of these are independent of the time if the initial pressure in the undisturbed medium p_0 is small compared with $\rho_0 \dot{R}_s^2$, which is of the order of the pressure being generated at the shock. This condition will certainly be met whenever the fluid-mechanical model is appropriate. Thus the question of whether a similarity solution is compatible with the boundary conditions depends solely on whether the form of the internal energy function F is such as to permit the time dependence to be eliminated from Eq. (26). Sedov[10] has pointed out that this can be done whenever the internal energy is of the form

$$e = p\,\varphi(\rho) \tag{27}$$

where $\varphi(\rho)$ is any function of the density. For such a case, Eq. (26) becomes

$$g(1,\theta) = \rho_0 f(1,\theta)\,\varphi\left[\rho_0 \psi(1,\theta)\right] \tag{28}$$

and all explicit time dependence is eliminated. Thus a self-similar solution is possible whenever the medium obeys the equation of state (27). In this case, the boundary values at the shock can be conveniently found by solving Eqs. (23)-(25) for ϕ, f, and g in terms of ψ

$$\phi(1,\theta) = f(1,\theta) = 1 - \frac{1}{\psi(1,\theta)} \tag{29}$$

$$g(1,\theta) = \frac{1}{2}\left[1 - \frac{1}{\psi(1,\theta)}\right]^2 \tag{30}$$

When these relations are substituted in Eq. (28), the result is an expression which can be solved for the density ratio at the shock

$$\frac{1}{2}\left[1 - \frac{1}{\psi(1,\theta)}\right] = \rho_0 \varphi\left[\rho_0 \psi(1,\theta)\right] \tag{31}$$

The fact that the density ratio is constant in the fundamental prerequisite for similarity. The other quantities at the shock are found from Eqs. (29) and (30).

From the point of view of application to shock propagation in solids, the most important implication of the similarity assumption is its restriction to state equations of a special kind. In the next Section we indicate the extent to which real materials are described by such a special family of state equations.

3. THE EQUATION OF STATE

For most solids, the equation of state approriate in the range of pressures generated during hypervelocity impact is the Mie-Grüneisen relation[11]

$$e(p,\rho) - e_c(\rho) = \frac{p - p_c(\rho)}{\rho\Gamma(\rho)} \tag{32}$$

where the subscript c denotes the cohesive contribution and where Γ is the Grüneisen constant, which depends weakly on ρ. The cohesive contributions can be found from measured shock wave data. Along the Hugoniot, Eq. (32) takes the form

$$e_H(\rho) - e_c(\rho) = \frac{p_H(\rho) - p_c(\rho)}{\rho\Gamma(\rho)} \tag{33}$$

Subtracting this from Eq. (32) then gives

$$e - e_H(\rho) = \frac{p - p_H(\rho)}{\rho\Gamma(\rho)} \tag{34}$$

The Mie-Grüneisen equation can be rearranged as

$$e = \frac{p}{\rho\Gamma(\rho)} - \Delta(\rho) \tag{35}$$

where

$$\Delta(\rho) = \frac{p_c(\rho)}{\rho\Gamma(\rho)} - e_c(\rho) = \frac{p_H(\rho)}{\rho\Gamma(\rho)} - e_H(\rho) \tag{36}$$

By comparison with Eq. (27), it can be seen that only the leading term of Eq. (35) can be accommodated in a self-similar solution. Such a solution will therefore be valid only when the pressure is sufficiently high that $\Delta(\rho)$

is small in comparison with the leading term. In fact, every impact will span a time interval during which this approximation fails. Furthermore, the pressures at which $\Delta(\rho)$ is too large to be neglected are nevertheless sufficiently high that the compressible-fluid approximation is still well justified. Thus the similarity solution can describe only the early phases of the fluid-dynamic process. A proper description at later times requires a nonsimilar solution which accounts for the presence of the term $\Delta(\rho)$. For the moment we defer this somewhat more difficult problem, and examine what can be done with the similarity solution itself, keeping in mind that it will apply only to the earlier stages.

Some of the theoretical analyses of shock waves in solid media[12] use the approximation that the state equation can be represented by that of a perfect gas with constant specific-heat ratio γ, namely

$$e = \frac{p}{(\gamma-1)\rho} \quad , \text{ i.e.,} \quad \varphi(\rho) = \frac{1}{(\gamma-1)\rho} \tag{37}$$

For this case, Eq. (31) reveals that the density ratio at the shock has the constant value

$$\psi(1,\theta) = \frac{\rho_1}{\rho_0} = \frac{\gamma+1}{\gamma-1}$$

The use of a perfect gas may be viewed as an approximation to the leading term of the Mie-Grüneisen equation, if the Grüneisen factor $\Gamma(\rho)$ is replaced by the constant value $\gamma-1$. This approximation, with γ chosen in the range from 2 to 4, amounts to a high-pressure approximation to the Mie-Grüneisen relation, and it makes available all the results of the extensive literature dealing with blast waves in perfect gases. It should be borne in mind, of course, that the similarity solution is not limited to the predictions made with a perfect gas model. The variation of Γ could be accounted for, but is neglected as a matter of convenience. When the perfect-gas approximation is made, the energy equation becomes

$$\frac{\partial p}{\partial t} + u\frac{\partial p}{\partial r} + \frac{w}{r}\frac{\partial p}{\partial \theta} + \frac{\gamma p}{\rho}\left(\frac{\partial \rho}{\partial t} + u\frac{\partial \rho}{\partial r} + \frac{w}{r}\frac{\partial \rho}{\partial \theta}\right) = 0 \tag{38}$$

In terms of the similar functions, this is

$$-2\frac{1-N}{N}f + (\phi - \eta)\left(\frac{\partial f}{\partial \eta} - \frac{\gamma f}{\psi}\frac{\partial \psi}{\partial \eta}\right) + \frac{\omega}{\eta}\left(\frac{\partial f}{\partial \theta} - \frac{\gamma f}{\psi}\frac{\partial \psi}{\partial \theta}\right) = 0 \tag{39}$$

In addition to this identification with the Mie-Grüneisen equation, a perfect-gas approximation may also be examined by seeing how accurately it represents the isentropes of a given material. This is done in Reference 13 for the case of iron, where it is shown that the approximation of a constant γ is satisfactory for describing the high-pressure states of iron as long as the function $\Delta(\rho)$ does not become significant.

Section 5 below gives a description of shock propagation due to hypervelocity impact, based on the perfect-gas approximation throughout. In Section 6, we present a solution which accounts for the influence of the nonsimilar term $\Delta(\rho)$ in an approximate way. In addition, Section 6 indicates work currently in progress, which properly accounts for the nonsimilar effect.

4. CONSERVATION OF ENERGY AND MOMENTUM

The total energy and momentum of the system must be conserved, as may be confirmed by forming the proper volume integral of the vector equations of motion, Eqs. (1) to (3). The actual integrals, whose values must be constant, may be derived as follows: Consider as the mass element a ring of volume $r\,dr\,d\theta \cdot 2\pi r \sin\theta$. The total energy E and momentum P are

$$\begin{aligned} E &= \int_0^{\pi}\int_0^{r_1(\theta)} \left[e + \tfrac{1}{2}\left(u^2 + w^2\right)\right]\cdot\rho\cdot 2\pi r^2 \sin\theta \; dr\,d\theta \\ &= 2\pi\rho_0 \dot{R}_s^2 R_s^3 \int_0^{\pi} \sin\theta \int_0^{\eta_1(\theta)} \left[g + \tfrac{1}{2}\left(\phi^2 + \omega^2\right)\right]\psi\eta^2 \, d\eta\, d\theta \end{aligned} \tag{40}$$

$$\begin{aligned} P &= \int_0^{\pi}\int_0^{r_1(\theta)} \left(u\cos\theta - w\sin\theta\right)\cdot\rho\cdot 2\pi r^2 \sin\theta \; dr\,d\theta \\ &= 2\pi\rho_0 \dot{R}_s R_s^3 \int_0^{\pi} \sin\theta \int_0^{\eta_1(\theta)} \left(\phi\cos\theta - \omega\sin\theta\right)\psi\eta^2 \, d\eta\, d\theta \end{aligned} \tag{41}$$

Here we encounter a fundamental difficulty. If we are to have a self-similar solution, the differential equations require $R_s = At^N$. However, a single value of N will not permit both of the relations above to be independent of time. Constancy of energy can be achieved only with $N = 2/5$, while momentum conservation requires $N = 1/4$, and in either case the parameter A is used to match the quantity being conserved. Thus it appears at first glance that a satisfactory solution cannot be achieved under the assumption of similarity. Reference 13 describes one method for overcoming this difficulty. The essence of the idea is that N is determined by a totally different consideration, and a second free parameter is introduced in such a way that both conservation conditions may be satisfied simultaneously.

It is clear, of course, that any solution which hopes to satisfy both conservation conditions simultaneously must make provision for mass ejection from the expanding crater. Consequently, a solution which supposes that the flow is one-half of a spherically symmetric disturbance (ignoring variations in the θ- direction) cannot satisfy momentum conservation. On the other hand, such solutions are considerably simpler than those which permit variations in the θ direction. In the remainder of this Section, we first describe the symmetric solution, and then take up the question of approximate solutions in which provision is made for mass ejection. An important conclusion emerges from the comparison of these two, namely, that the vastly simpler spherically-symmetric solution is for practical purposes identical with the more complicated solution which allows for mass ejection.

When the flow is spherically symmetric, ω and all derivatives with respect to θ vanish, and the similarity equations become ordinary differential equations. Denoting the ordinary derivative with respect to η by a prime, these are

$$(\phi-\eta)\psi' + \psi\left(\phi' + 2\frac{\phi}{\eta}\right) = 0 \tag{42}$$

$$-\frac{1-N}{N}\phi + (\phi-\eta)\phi' + \frac{f'}{\psi} = 0 \tag{43}$$

$$-2\frac{1-N}{N}f + (\phi-\eta)\left(f' - \frac{\gamma f}{\psi}\psi'\right) = 0 \tag{44}$$

The parameter γ may be thought of as related to the Grüneisen constant, as mentioned earlier. These equations may be solved explicitly for the derivatives in the form

$$\psi' = \frac{-(\phi-\eta)^2 \frac{2\psi\phi}{\eta} + 2\frac{1-N}{N} f - \frac{1-N}{N}\psi\phi(\phi-\eta)}{(\phi-\eta)\left[(\phi-\eta)^2 - \gamma f/\psi\right]} \tag{45}$$

$$\phi' = \frac{\frac{1-N}{N}\phi(\phi-\eta) + \frac{\gamma f}{\psi}\frac{2\phi}{\eta} - 2\frac{1-N}{N}\frac{f}{\psi}}{(\phi-\eta)^2 - \frac{\gamma f}{\psi}} \tag{46}$$

$$f' = \frac{f\left\{(\phi-\eta)\left[2\frac{1-N}{N} - \frac{2\gamma\phi}{\eta}\right] - \gamma\frac{1-N}{N}\phi\right\}}{(\phi-\eta)^2 - \frac{\gamma f}{\psi}} \tag{47}$$

From Eqs.(37), (23)-(26), the boundary conditions at the shock can be found as

$$\phi(1) = f(1) = \frac{2}{\gamma+1} \quad ; \quad \psi(1) = \frac{\gamma+1}{\gamma-1} \tag{48}$$

Equations (45) to (48) (with $N = 2/5$) were first presented by G. I. Taylor[14] who worked out a few numerical and approximate analytical solutions for γ ranging from 1.2 to 1.67, the range appropriate for gases. Subsequently, an analytic solution (also with $N = 2/5$) was published independently by J. L. Taylor[15], Latter [16], and Sakurai[17]. Simultaneously with G. I. Taylor's work, Sedov[10] had also found this analytic solution.

The parameter N must be specified before solutions of these equations can be found. It appears that physically acceptable solutions exist only when $N = 2/5$, a value which conserves the total energy, as noted above. When N

is taken to be different from 2/5, the solution exhibits infinite slopes. Reference 13 presents results typical of those found in the range $.25 < N < .4$ when a solution of this sort is attempted. This nonexistence of symmetric solutions apparently explains the difficulty encountered by Davids et al[18] in attempting to find a spherically symmetric solution for constant momentum.

In what follows, N is chosen as 2/5, and the terms "constant-energy" and "spherically symmetric" are used interchangeably in referring to the solution.

Solutions of these equations for γ in the range from 2 to 20 are presented in Reference 13. Figures 1 and 2 show typical results, for the cases $\gamma = 3$ and $\gamma = 16$. These figures display the usual feature that the [illegible] drops off rather sharply behind the shock, indicating that most of the [illegible] is concentrated near the shock. For $\gamma > 7$, a cavity begins to fo[illegible] values of γ, as pointed out by Sedov[10], and the particle velocities show a marked increase near the edge of the cavity.

The problem of obtaining solutions when [illegible] is included as an independent variable is considerably more difficult. The basic equations are partial differential equations and, as pointed out in Reference 13, they are of mixed character, containing both elliptic and hyperbolic regions. Furthermore, they must meet a zero-pressure boundary condition along a line whose location is unknown in advance. To make matters worse, the differential equations contain a parameter N whose value is unspecified. No attempt has been made to solve these equations; instead, partial solutions are sought by restricting attention to conditions along the axis of symmetry. In this way we can learn a great deal about the solution with relatively little effort. Along the axis of

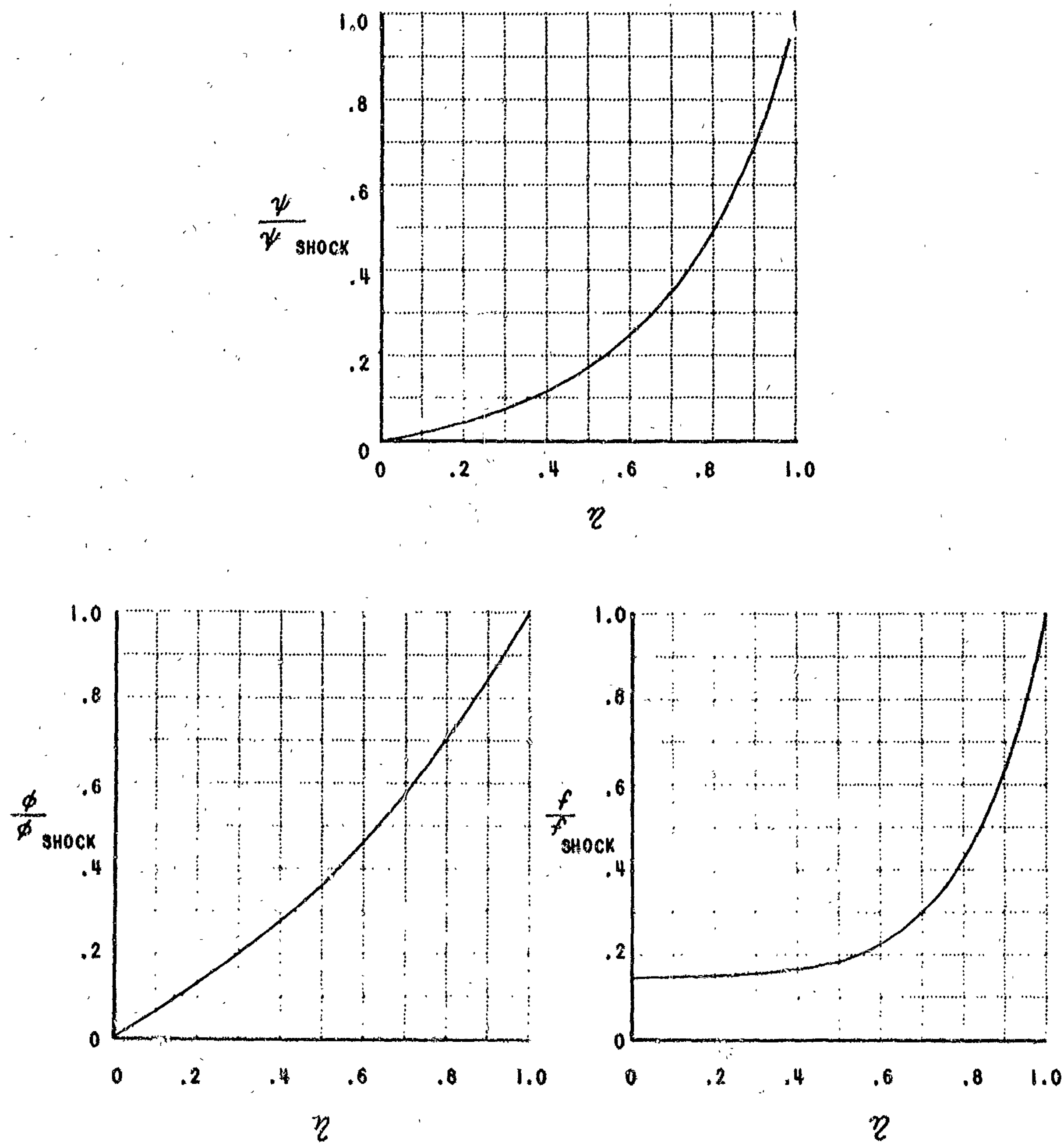

Figure 1 DISTRIBUTION OF DENSITY, PARTICLE VELOCITY, AND PRESSURE
CONSTANT-ENERGY, SPHERICALLY-SYMMETRIC BLAST WAVES
$\gamma = 3$

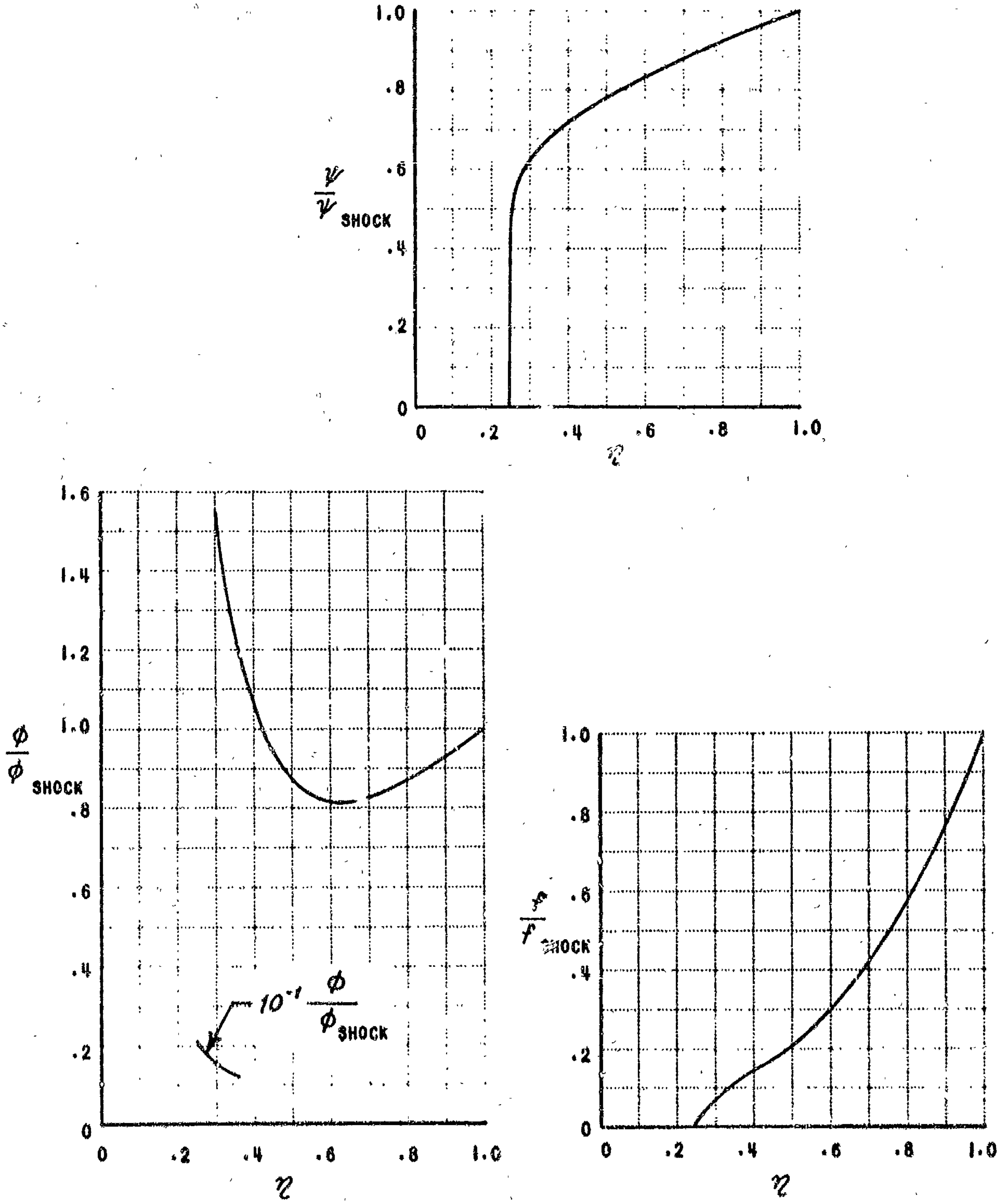

Figure 2 DISTRIBUTION OF DENSITY, PARTICLE VELOCITY, AND PRESSURE CONSTANT-ENERGY, SPHERICALLY-SYMMETRIC BLAST WAVES

$\gamma = 16$

symmetry

$$\theta = 0, \quad 0 \le \eta \le 1 \quad ; \quad \theta = \pi, \quad 0 \le \eta \le \infty$$

the similarity equations take the form

$$(\phi - \eta)\psi' + \psi\left(\phi' + \frac{\tau}{\eta} + 2\frac{\phi}{\eta}\right) = 0 \tag{49}$$

$$-\frac{1-N}{N}\phi + (\phi - \eta)\phi' + \frac{f'}{\psi} = 0 \tag{50}$$

$$-2\frac{1-N}{N}f + (\phi - \eta)\left(f' - \frac{\gamma f}{\psi}\psi'\right) = 0 \tag{51}$$

where primes indicate ordinary derivatives with respect to η, and where the quantity $\tau(\eta)$ is given by

$$\tau(\eta) = 2\,\frac{\partial \omega}{\partial \theta}(\eta, 0) \tag{52}$$

(The factor 2 originates from the contribution of the term $\omega \cot \theta$.) Except for the presence of τ in Eq. (49), these are identical with the Taylor equations for a spherically symmetric disturbance, discussed above. The function $\tau(\eta)$ represents the influence of off-axis conditions, as must be expected whenever a partial differential equation is specialized to a single line in the plane of its independent variables. The boundary conditions at the shock are

$$\phi(1) = f(1) = \frac{2}{\gamma+1} \quad ; \quad \psi(1) = \frac{\gamma+1}{\gamma-1} \quad ; \quad \tau(1) = 0 \tag{53}$$

Equations (49) to (51) may be solved explicity for the derivatives in the form

$$\psi' = \frac{-(\phi-\eta)^2\left(\frac{2\psi\phi}{\eta} + \frac{\psi\tau}{\eta}\right) + 2\frac{1-N}{N}f - \frac{1-N}{N}\psi\phi(\phi-\eta)}{(\phi-\eta)\left[(\phi-\eta)^2 - \gamma f/\psi\right]} \tag{54}$$

$$\phi' = \frac{\frac{1-N}{N}\phi(\phi-\eta) + \frac{\gamma f}{\psi}\left(\frac{2\phi}{\eta} + \frac{\tau}{\eta}\right) - 2\frac{1-N}{N}\frac{f}{\psi}}{(\phi-\eta)^2 - \gamma f/\psi} \tag{55}$$

$$f' = \frac{f\left\{(\phi-\eta)\left[2\frac{1-N}{N} - \gamma\left(\frac{2\phi}{\eta} + \frac{\tau}{\eta}\right)\right] - \gamma\frac{1-N}{N}\phi\right\}}{(\phi-\eta)^2 - \frac{\gamma f}{\psi}} \tag{56}$$

These obviously have a singularity at the point where the denominator vanishes. This quantity is the special case, for $\omega = 0$, of the function discussed in Reference 13, whose sign determines whether the partial differential equations (19), (21), (39), have elliptic or hyperbolic character. The point on the axis of symmetry where the denominator changes sign corresponds to the intersection of this line with the axis. In order that the solution may pass smoothly through this point, the numerators in Eqs. (54) to (56) must also vanish there. Reference 13 points out that such a condition is achieved if the function

$$H(\eta) = (\phi-\eta)\left\{\frac{2}{\gamma}\frac{1-N}{N} - \frac{2\phi}{\eta} - \frac{\tau}{\eta}\right\} - \frac{1-N}{N}\phi$$

vanishes at the same point.

The function $\tau(\eta)$ cannot be chosen arbitrarily. Thus the only parameter that can be used to guarantee a smooth crossing of the sonic point is N, and this consideration forms the criterion for the choice of N. For each γ, and a specification of $\tau(\eta)$, N is chosen so as to provide a continuous transition through the singularity. Thus N will in general be a function of γ. It should be noted in passing that this problem never comes up in the spherically-symmetric, constant-energy case. There the vanishing of the denominator always coincides with either the origin (for $\gamma < 7$), or with the edge of the cavity (for $\gamma > 7$), and the entire flow field is elliptic in that solution.

In order to actually obtain a smooth crossing of the singularity, Eqs. (54) to (56) must be solved for various values of N (and given γ) until such a crossing is found. Before such an integration can be done, $\tau(\eta)$ must be specified. However, no rigorous determination of $\tau(\eta)$ and with it $N(\gamma)$, can be made without solving the full partial differential equations. Approximations to N may be found by approximating τ and then integrating Eqs. (54) to (56). Instead of approximating τ itself, one may instead relate τ to other physical quantities which may be approximated more easily. In particular, by differentiating Eq. (21) with respect to θ; and then specializing for the axis of symmetry, one finds

$$-\frac{1}{2}\,\frac{1-N}{N}\,\tau+\frac{1}{2}(\phi-\eta)\tau'+\frac{\tau^2}{4\eta}+\frac{\phi\tau}{2\eta}+\frac{1}{\eta\psi}\,\frac{\partial^2 f}{\partial\theta^2}(\eta,0)=0 \qquad (59)$$

from which it is seen that approximations to the pressure distribution can be used to generate corresponding approximations to τ'. This process can be continued, of course, by taking higher-order derivatives, with respect to θ, of any of the equations of motion. Each of the resulting expressions will contain at least one unknown function, so the utility of the procedure is dictated by one's ability to approximate the unknown function. For this purpose, Eq. (57) is especially useful. At the shock, the pressure is uniform, while behind the shock it begins to decrease. The rate of decrease is faster near $\theta=\pm\frac{\pi}{2}$, as the influence of the vacuum outside the developing crater makes itself felt. Qualitatively, the pressure distribution would be expected to have the appearance

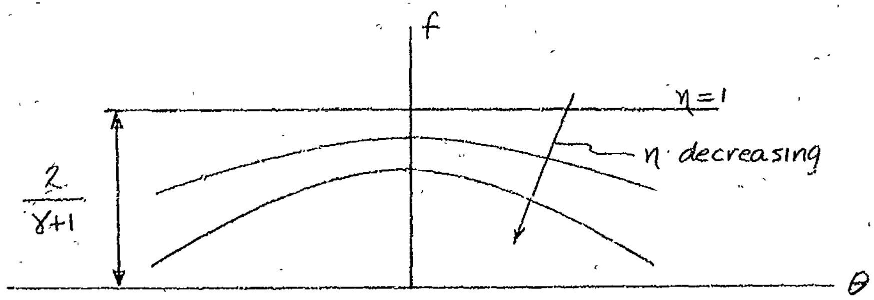

The quantity $\frac{\partial^2 f}{\partial \theta^2}(\eta, 0)$, which is essentially the curvature of these lines at $\theta = 0$, will be zero at the shock and will become negative with increasing magnitude as η falls below one. Such considerations suggest the approximation

$$\frac{\partial^2 f}{\partial \theta^2}(\eta, 0) = -K(1-\eta)^a f(\eta, 0) \tag{58}$$

where K and a are constants. Crudely, one may think of this approximation as fitting a cosine variation to the curves above, with a multiplicative function of η introduced in such a way as to guarantee zero curvature at the shock.

The constants a and K must be chosen so as to yield values of τ which are at most of the same order as that of ϕ.

Figure 3 shows results which have been found for the case $a = 1$, and $K = 10$. For a given value of γ, and selected values of N, the equations are integrated by a Runge-Kutta procedure, starting from the shock values given in Eq. (53). A smooth crossing of the singularity is achieved with the value $N = .375$, and the distributions of density, particle velocity, pressure and the function τ are shown in the figure. The results given here are typical of those which occur for other values of γ. In addition, some calculations have been made with $K = 1$, and the results are not far different from those

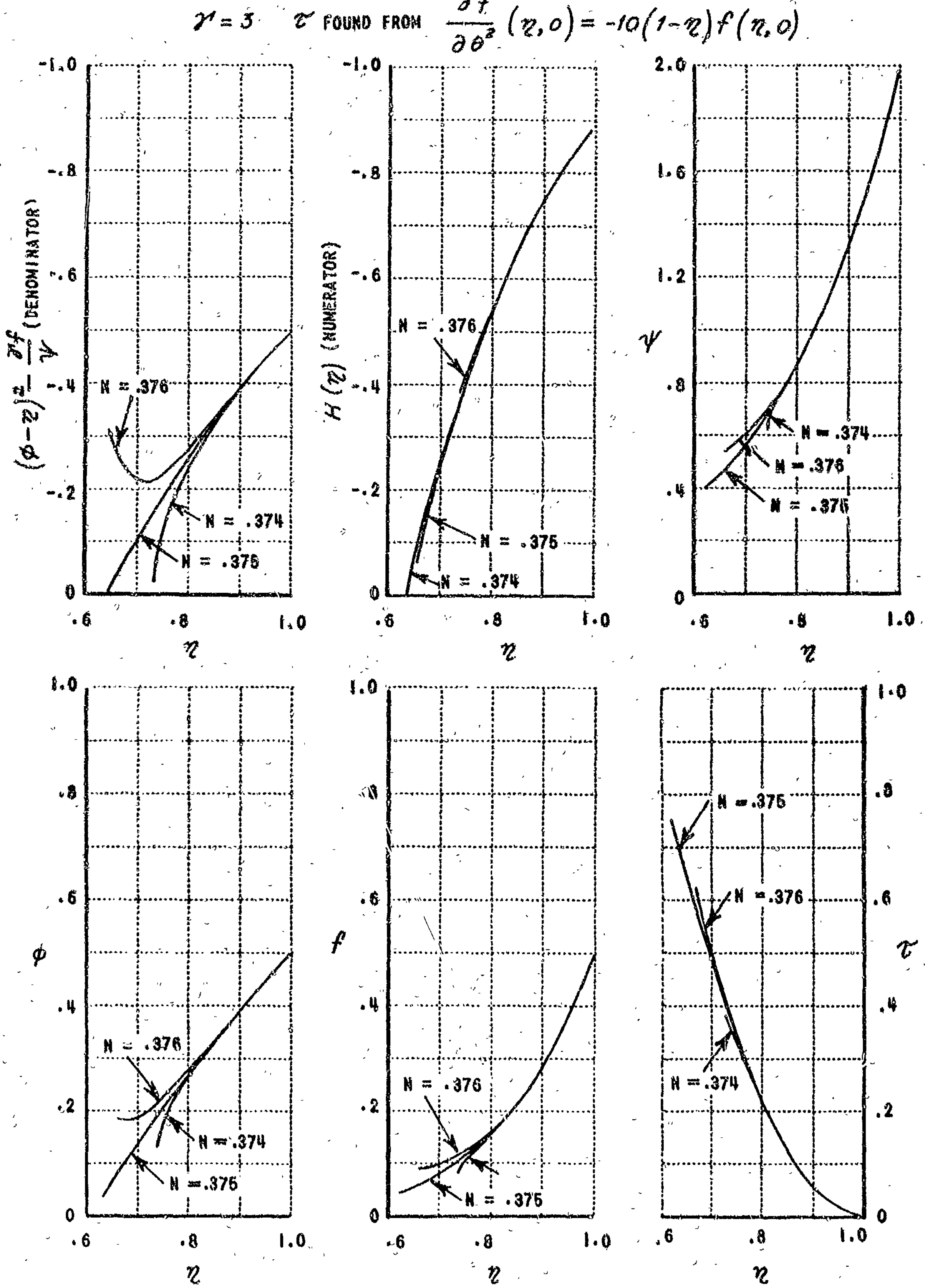

Figure 3 CENTERLINE DISTRIBUTIONS OF DENSITY, PRESSURE, AND VELOCITY

shown here.

In general, it is found that values of $\mathcal{N}$ corresponding to a smooth crossing of the singularity are quite close to the value 2/5 that applies for the symmetric, constant-energy solution. Furthermore, the quantity τ does not attain an appreciable value until some distance away from $\eta = 1$, where the density has fallen to a low value. Thus we might expect that, near the shock at least, these solutions will not differ greatly from the constant-energy solution. This is indeed the case. Figure 4 compares the two types of solution for $\gamma = 3$ and shows that, along the centerline at least, the motion of most of the mass involved is well approximated by the solution for $\mathcal{N} = 2/5$. One may expect this trend to persist even for $\theta > 0$, suggesting that the Taylor solution will in general be an excellent approximation to the considerably-more-complicated-asymmetric solution. The comparison shown in this figure is typical of the results found at other values of γ.

So far as blast-wave theory is concerned, then, the energy of the projectile plays the dominant role, its momentum being of only secondary importance. In assessing the significance of this finding, it is well to bear in mind three different flow models that might be considered. In addition to the two described above, it is also possible, in principle, to find a solution in which provision is made for mass ejection, but which has zero net momentum:

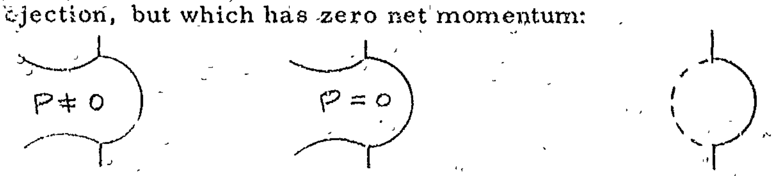

symmetric model

Our conclusion about the relative unimportance of momentum conservation requires only that the first two of these models give nearly identical predictions. The fact is that we find close similarity to the correct flow pattern

$\gamma = 3$ SOLUTION FOR N = 0.375 BASED ON THE APPROXIMATION

$$\frac{\partial^2 f}{\partial \theta^2}(\eta, 0) = -10(1-\eta) f(\eta, 0)$$

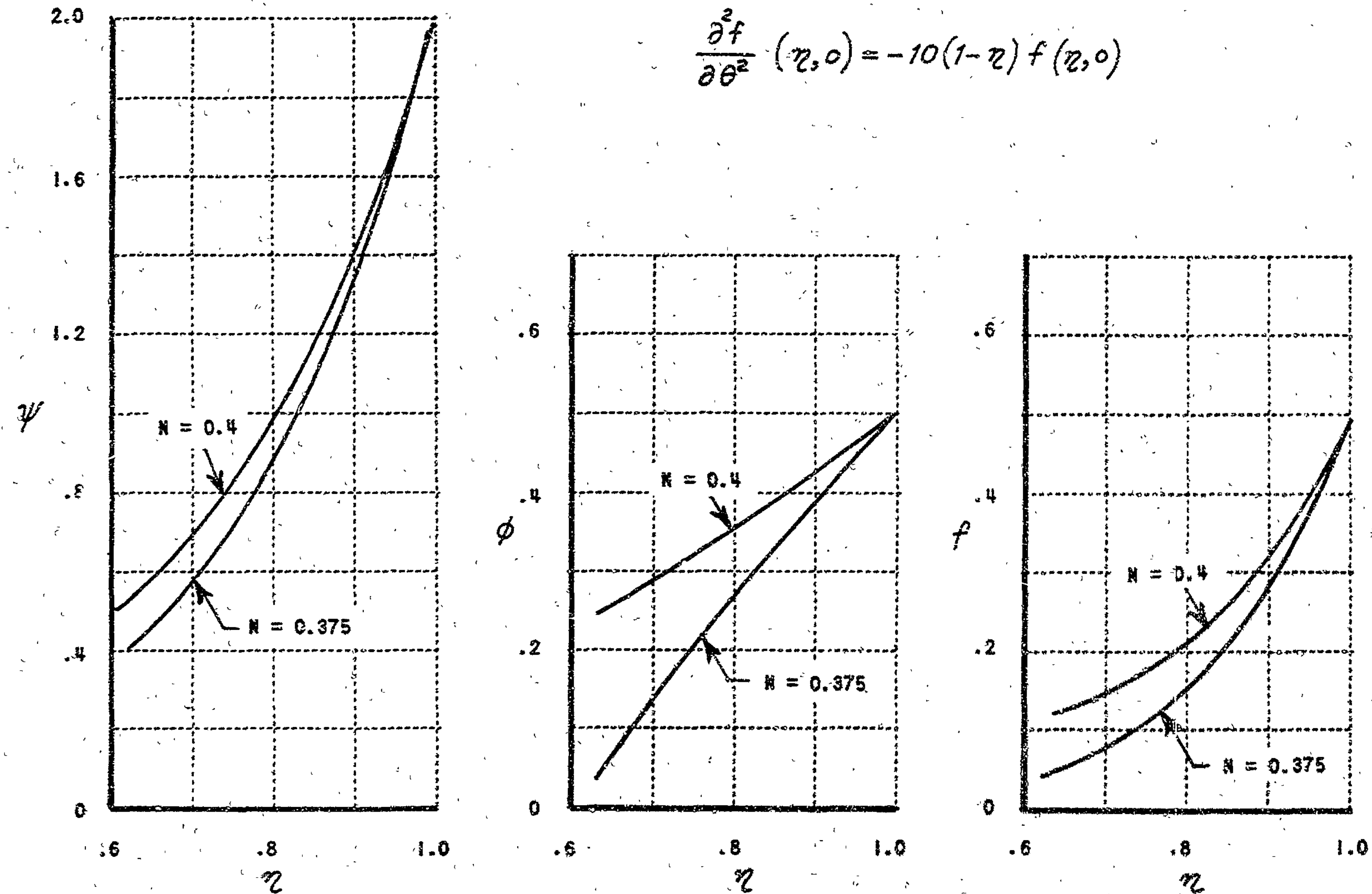

Figure 4 CONSTANT-ENERGY, SPHERICALLY-SYMMETRIC SOLUTION (N = 0.4) COMPARED WITH "CENTERLINE" SOLUTION (N = 0.375)

even for the Taylor solution, in which the momentum varies as a function of time.

One plausible physical explanation is based on the experimental observation[19] that targets struck by hypervelocity projectiles often acquire momenta many times that of the projectile, implying that the material ejected from the target must also carry several times the projectile momentum. Thus it appears that the momentum of the projectile itself makes only a minor contribution to the over-all conservation process.

A corrolary of this conclusion is that the conditions of hypervelocity impact can be simulated by any experiment which duplicates the energy of the incident particle, irrespective of whether its momentum is correctly matched. In particular, any intense source of short-pulse electromagnetic radiation, such as the output of some currently available lasers, should be capable of providing such a simulation. Such an experimental technique appears to hold promise, and the basis for it is discussed in some detail in the Appendix.

It is important to keep in mind that the predominant importance of energy, as revealed by these solutions, does not necessarily imply that crater volume will be scaled by the projectile energy. Actually, energy scaling is a feature which applies only to the rate of propagation of the shock wave itself. A description of the variation of crater size with various parameters of the impact process requires that the solution for shock radius be converted into a prediction of crater size. Whether the final result of such a process (which presumably will call material strength into play) will still be scaled by the energy of the process, is a question that is unresolved at this point.

As a final word of caution, it must be emphasized that our present data concerning the unimportance of momentum conservation are restricted to the similarity, or strong-shock limit. It remains to be determined whether the same results will be found at lower pressures, where the nonsimilar nature of the problem must be considered.

In the next two Sections, we restrict our attention to solutions in which only the energy is conserved. Thus, the solutions are spherically symmetric. These solutions are used to develop an expression for the rate of shock propagation as a function of the kinetic energy of the impacting particle.

5. TAYLOR SOLUTION FOR SHOCK PROPAGATION

This Section reviews the well-known solution for a spherical blast wave in a perfect gas, in order to provide a background for the quasi-steady solution presented in the next section. By using the constant-energy distributions of pressure, density, and particle velocity described in the Section above, an explicit description of the shock propagation can now be given if the total energy E of the system is specified. The sum of the internal and kinetic energy of the fluid set into motion is given by the intergral over a hemisphere

$$\begin{aligned} \int_0^{R_s} \left(e + \tfrac{1}{2}u^2\right) 2\pi\rho r^2 dr &= \int_0^{R_s} \left(\frac{1}{\gamma-1}\frac{p}{\rho} + \frac{1}{2}u^2\right) 2\pi\rho r^2 dr \\ &= 2\pi\rho_0 R_s^3 \dot{R}_s^2 \, I_1(\gamma) \end{aligned} \tag{59}$$

where

$$I_1(\gamma) = \int_0^1 \left(\frac{1}{\gamma-1}\frac{f}{\psi} + \frac{1}{2}\phi^2\right)\psi\eta^2 d\eta \tag{60}$$

This integral has been evaluated for the values of γ mentioned above, by substituting in Eq. (60) the analytical solution. The results are shown in Figure 5.

If the total energy E is now specified, a simple differential equation for $R_s(t)$ results

$$E = 2\pi\rho_0 R_s^3 \dot{R}_s^2 \, I_1(\gamma) \tag{61}$$

The term $2\pi\rho_0 R_s^3$ is three times the target mass processed up to the time t. Thus, $3\,I_1(\gamma)$ may be thought of as a dimensionless coefficient giving the ratio of the mass-averaged value of $e+\frac{1}{2}u^2$ to the quantity $\dot{R}_s^2$,

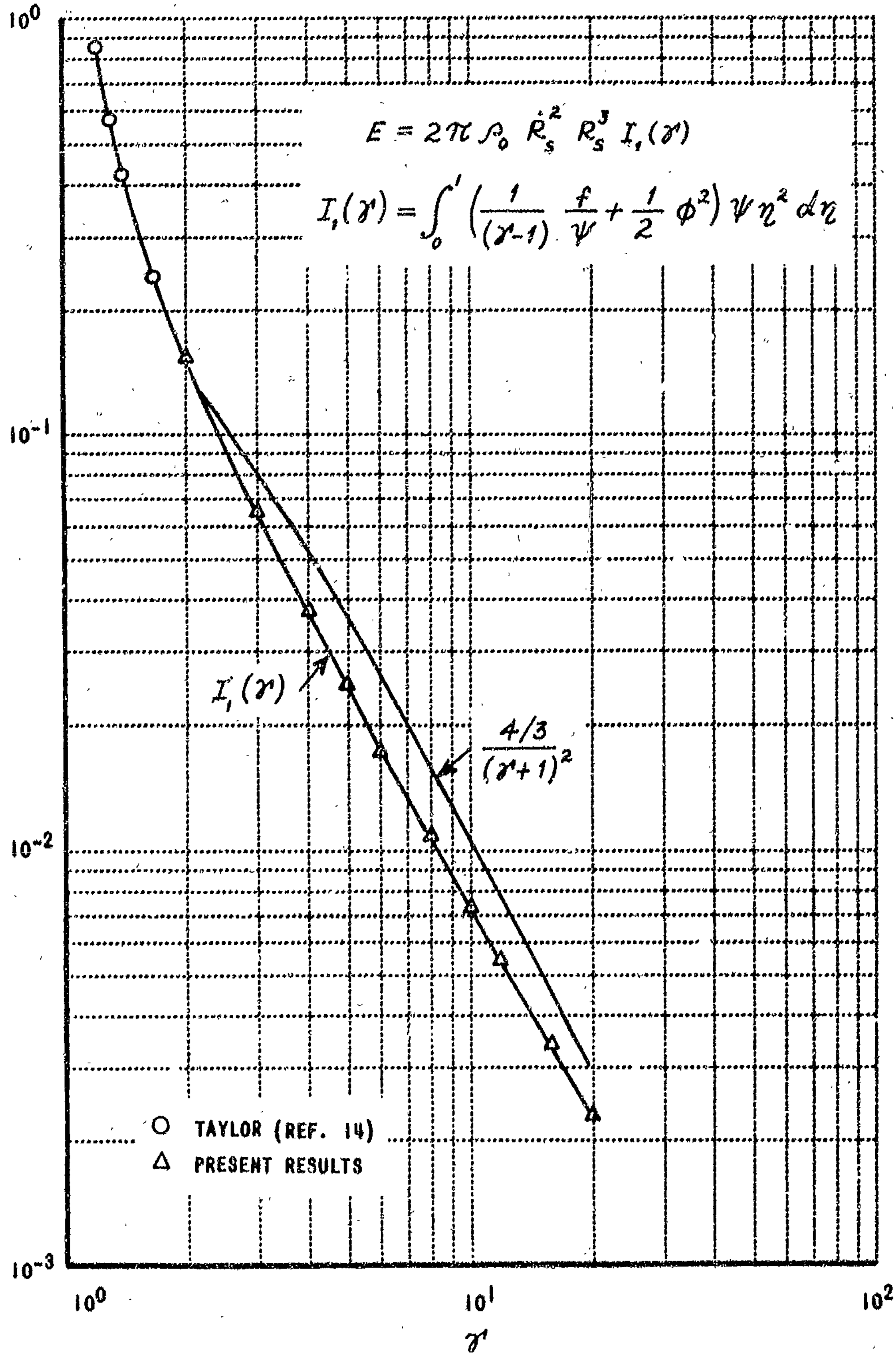

Figure 5 THE FUNCTION $I_1(\gamma)$ FOR SPHERICALLY-SYMMETRIC BLAST WAVES

i.e.

$$3I_1(\gamma) = \frac{E/\frac{2}{3}\pi\rho_0 R_s^3}{\dot{R}_s^2} = \frac{\left(e+\frac{1}{2}u^2\right)_{AVG.}}{\dot{R}_s^2} \tag{62}$$

Since $\dot{R}_s^2$ is proportional to the energy at the shock

$$\dot{R}_s^2 = \frac{(\gamma+1)^2}{4}\left(e+\frac{1}{2}u^2\right)_{SH} \tag{63}$$

we obtain

$$I_1(\gamma) = \frac{4}{3(\gamma+1)^2}\,\frac{\left(e+\frac{1}{2}u^2\right)_{AVG.}}{\left(e+\frac{1}{2}u^2\right)_{SH}} \tag{64}$$

Because most of the mass is concentrated near the shock, the mass-averaged value of any quantity is very nearly its value at the shock. Thus the factor $4/3(\gamma+1)^2$ is a good approximation to I_1, as shown in Figure 5. This factor originates from Eq. (63), which states that, the larger the value of γ, the larger must be the shock speed if a given energy per unit mass is to be achieved behind the shock. We may attach the same significance to $I_1(\gamma)$: if a given energy is to be distributed in two materials for which the γ's differ, the shock speed will have to be greater in the material having the larger γ.

The solution of Eq. (61) is the classical Taylor solution for a strong blast wave

$$R_s(t) = \left(\frac{25}{8\pi I_1(\gamma)}\,\frac{Et^2}{\rho_0}\right)^{1/5} \tag{65}$$

Here the influence of γ is shown more clearly. For a given E and ρ_0, the shock radius will grow more rapidly for large values of γ.

To apply Eq. (65) to a given case, the total energy E and the value of the parameter γ must be specified. In all the applications made below, this energy is taken to be the kinetic energy of the impacting particle. The value of γ is associated with the magnitude of the Grüneisen factor, Γ, and hence it would be expected to lie in the range from, say, 2 to 3. Values even larger than this might be considered, especially in the range where the function $\Delta(\rho)$ is too large to be neglected. Reference 13 makes application to problems in which γ is chosen to be as large as 20, in an effort to match the full Mie-Grüneisen equation.

6. QUASI-STEADY SOLUTION FOR SHOCK PROPAGATION

The similarity solution described above will be valid only in the limit of extremely high pressure, where the density ratio across the shock is constant. In an actual impact, however, such a condition is not met, especially during the later stages of the cratering process, when the shock strength begins to decay toward that of a stress wave.

Thus a proper description of shock propagation in real materials calls for an analysis in which the nonsimilar features of the problem are correctly accounted for. Analyses of this sort have been done for gases, with varying degrees of approximation. Notable among these is the perturbation method, explored by Sakurai[20], among others. Applied to the present problem, the perturbation analysis would seek the first-order departure from similarity, for the case where $\Delta(\rho)$ is small, but not negligible, compared with $p/\rho\Gamma(\rho)$. A more powerful approach, valid over a wider range of pressure, has been developed by Oshima[21], who calls it the "Quasi-Similarity" solution. The essence of his method is to solve the problem for a range of values of the shock Mach number M, defined as $\dot{R}_s/c$, where c denotes the target sound speed. For each value of M, the correct boundary values are used at the shock, and certain terms are included in the differential equations to approximate the nonsimilar effect. The analysis leads to a solution for the shock Mach number as a function of time, starting from the blast-wave limit ($M = \infty$) and tending toward the acoustic limit ($M = 1$) at large time. At each instant, the distributions of pressure, density, etc., are given, once the shock Mach number is known. For air, Oshima's solution agrees well with experimental observation and with machine solutions, both in regard to the shock propagation, and to the distributions behind the shock.

Oshima's method is being applied to the propagation of shock waves in solid media, but the results are incomplete. As an interim solution, we have worked out an analogous, but more approximate description of the shock propagation, which we shall identify by the term "Quasi-Steady." We assume that the distributions of pressure, density, etc., at any shock speed are the same as the self-similar, perfect-gas distributions which would have the same values at the shock. Thus, at the instant when the shock speed is such as to create a density ratio at the shock of 1.5, the solution is assumed to be the self-similar solution for $\gamma = \frac{1.5+1}{1.5-1} = 5$; when $\rho_1/\rho_0 = 1.4$, the solution is assumed to be that for $\gamma = 6$, etc. Thus the right values at the shock are always used (as is the case in Oshima's work), but the distributions behind the shock are not correct. However, the quasi-similar distributions for air[22] at moderate shock Mach numbers show a qualitative resemblance to the present results[13] for γ in the range from 2 to 20. Thus, because most of the mass is concentrated near the shock, we may expect the quasi-steady solution to be a useful approximation.

The starting point for the analysis is the energy-balance integral

$$E = 2\pi \rho_0 R_s^3 \dot{R}_s^2 I_1(\gamma) \tag{66}$$

In a similarity solution, γ is taken to be a constant, related to the Grüneisen factor. We now propose to allow γ to vary, so as to match conditions at the shock at each instant. This is very simple for a large number of materials, whose Hugoniots are well approximated over a wide range[11] by

$$u_s = c + S u_1 \tag{67}$$

For such a material, γ is related to the shock speed by

$$\gamma = \frac{\rho_1/\rho_0 + 1}{\rho_1/\rho_0 - 1} = \frac{(2s-1)\frac{\dot{R}_s}{c} + 1}{\frac{\dot{R}_s}{c} - 1} \tag{68}$$

Use of this in Eq. (66) leads to a simple relation between shock speed and shock radius. Defining a length scale R_0 by

$$R_0 = \left(\frac{E}{2\pi\rho_0 c^2}\right)^{1/3} \tag{69}$$

equation (66) can be rewritten in the dimensionless form

$$\frac{R_s}{R_0} = \left\{\frac{1}{\left(\frac{\dot{R}_s}{c}\right)^2 I_1\left[\gamma\left(\frac{\dot{R}_s}{c}; s\right)\right]}\right\}^{1/3} \tag{70}$$

Figure 6 shows this relation for $s = 1.2$, 1.5, and 2.0. It is important to note that the shock speed approaches c when R_s becomes large, because as $\dot{R}_s \to c$, $\gamma \to \infty$, and $I_1 \to 0$. Thus the quasi-steady solution tends toward the acoustic, or stress-wave limit, at large time. Figure 7 shows a comparison of Eq. (70) with the experiments of Fraiser and Karpov[8]. The exact value of s for the target is probably somewhere in the range from 1.2 to 2, and theoretical predictions for both values are shown. The data, which lie quite close to the stress-wave velocity, are well predicted by the quasi-steady theory.

By using Eq. (70) to give $\dot{R}_s$ as a function of R_s, a simple solution for the shock trajectory can be found from the identity

$$\frac{ct}{R_0} = \int_0^{R_s/R_0} \frac{c}{\dot{R}_s}\, d\left(\frac{R_s}{R_0}\right) \tag{71}$$

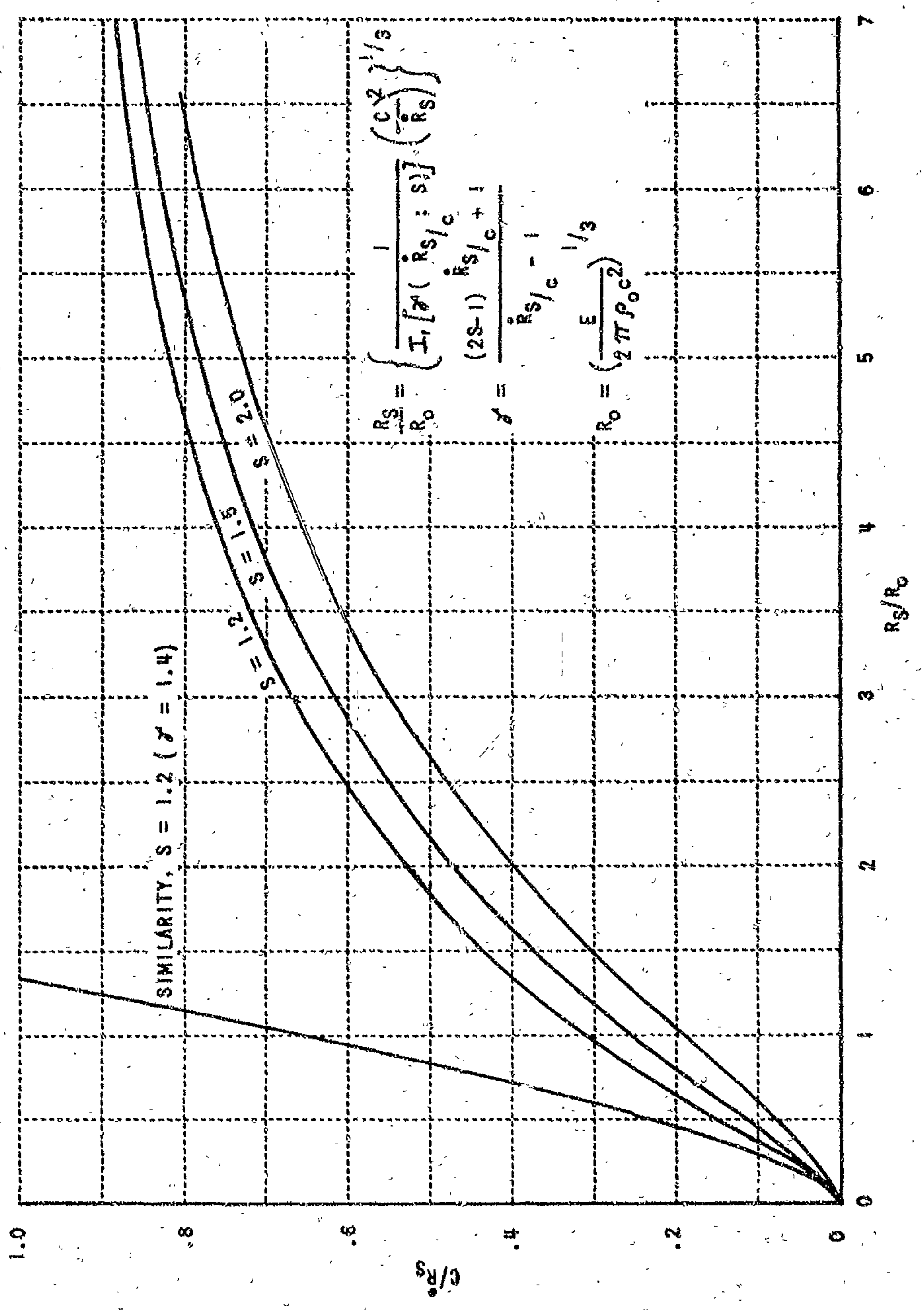

Figure 6 SHOCK SPEED - SHOCK RADIUS RELATION FOR "QUASI-STEADY" SOLUTION

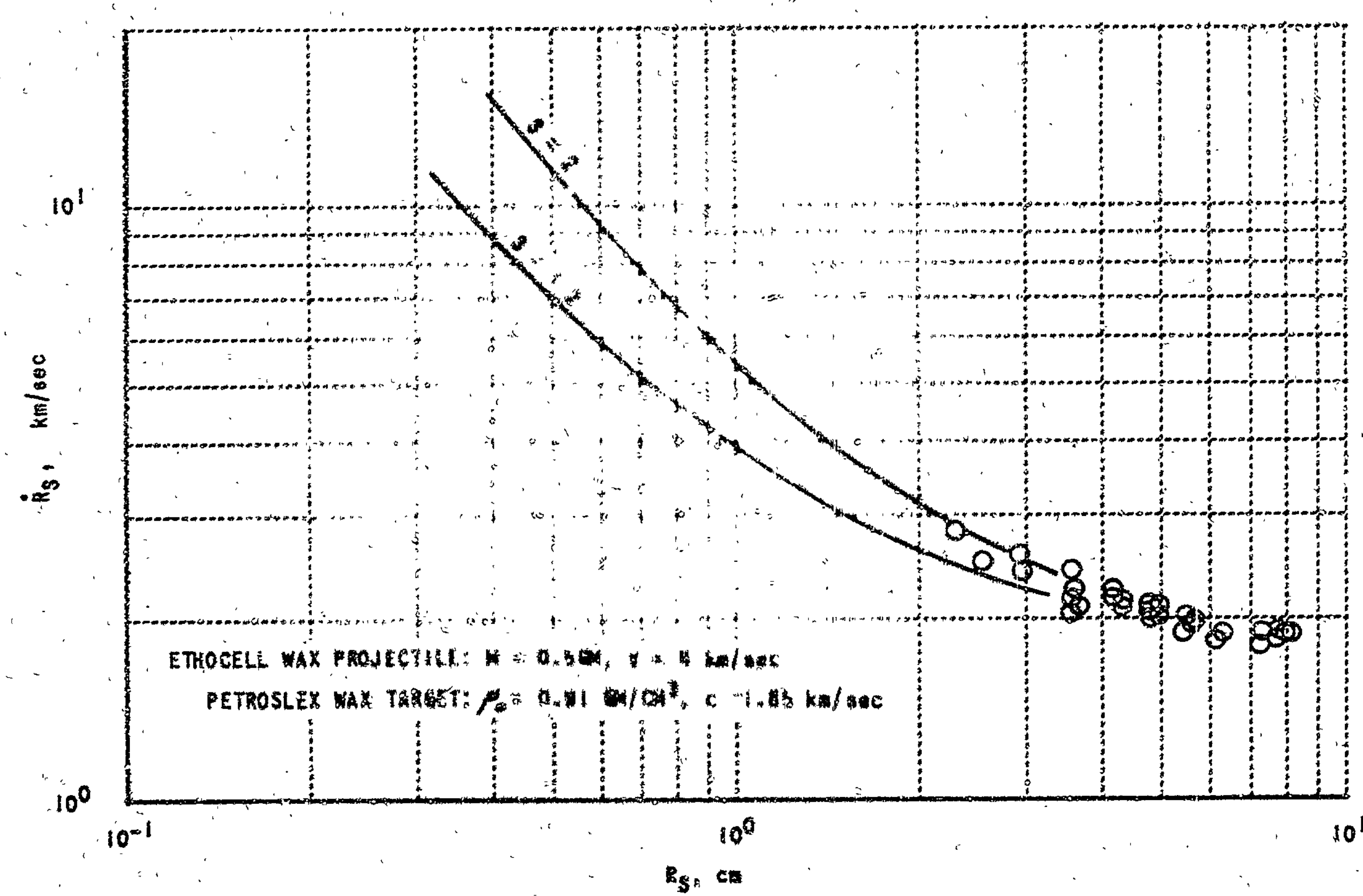

Figure 7 QUASI-STEADY PREDICTION OF SHOCK SPEED - SHOCK RADIUS RELATION COMPARED WITH DATA OF FRASIER & KARPOV

Figure 8 shows this relation for the three values of S mentioned before. Larger values of S are associated with faster shock propagation, a manifestation of the same phenomenon as that due to γ in the perfect-gas approximation. Also shown on this figure are the experimental data of Eichelberger and Gehring[6] and of Halperson and Hall[7] for a Lucite target, as well as the shock histories calculated by Bjork for iron striking Tuff[2], and for iron striking iron[1]. The agreement found here, over such a wide range of impact conditions, indicates that the quasi-steady theory is a useful apporximation, especially at times greater than R_0/c. Of course, in the early stages of the impact process before the projectile has been destroyed, the shock propagates at a constant speed. It is only after this early phase that our approximation of an instantaneous point-release of energy becomes valid. We may in general expect the measured trajectories to begin with a constant-speed phase $(R_s \propto t)$, followed by a transition to a power-law behavior $(R_s \propto t^N)$, with N between .40 and 1.0, depending on the duration of the impact phase. This exponent increases toward 1.0 again at large time, as the (constant) stress-wave speed is approached. For ct/R_0 greater than about 1.0, the correlation of Fig. 8 is quite good, although some scatter is still present. There is not enough data, at present, to determine whether this remaining scatter represents an additional impact-speed dependence, or whether it is simply an effect of S not properly accounted for by the quasi-steady theory. The application of Oshima's method, currently in progress, will shed considerable light on this question by properly accounting for the influence of the state equation, but there is obviously a great need for further measurements of shock-wave trajectories,

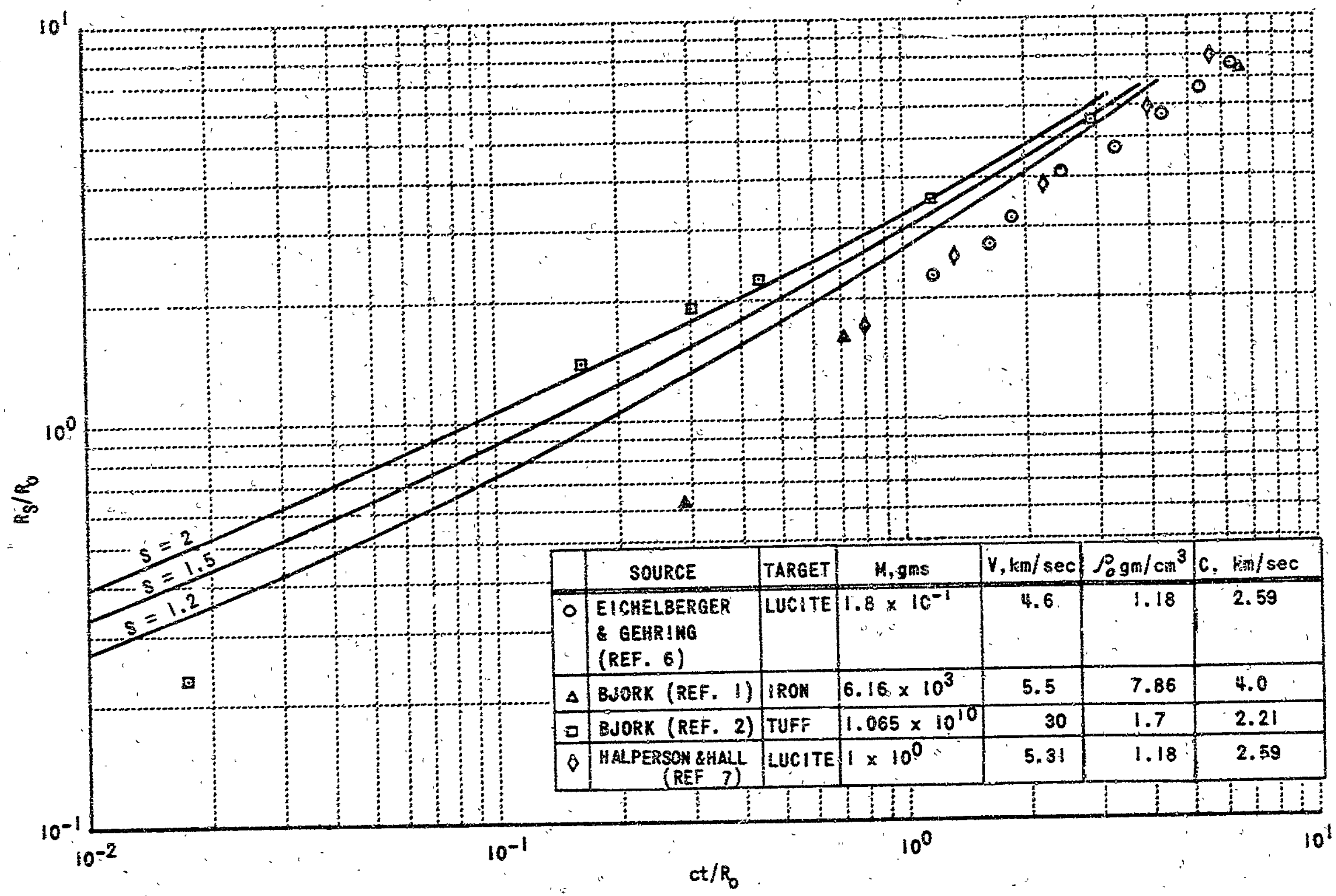

	SOURCE	TARGET	M, gms	V, km/sec	ρ_o gm/cm^3	C, km/sec
○	EICHELBERGER & GEHRING (REF. 6)	LUCITE	1.8×10^{-1}	4.6	1.18	2.59
△	BJORK (REF. 1)	IRON	6.16×10^3	5.5	7.86	4.0
□	BJORK (REF. 2)	TUFF	1.065×10^{10}	30	1.7	2.21
◊	HALPERSON & HALL (REF 7)	LUCITE	1×10^0	5.31	1.18	2.59

Figure 8 QUASI-STEADY SOLUTION FOR SHOCK TRAJECTORY

especially in metals.

It has been observed[6] that the characteristic time for shock propagation in Lucite is considerably shorter than the time during which material is ejected from an aluminum or lead target, under identical impact conditions, and the difference is sometimes attributed to the dynamic strength of the plastic at high strain rate. In this regard, it is interesting to note in Fig. 8 the close correlation between Bjork's calculations in iron ($S \approx 1.6$) and the experimental observations in Lucite ($S \approx 1.5$), all at approximately 5 km/sec. This correlation indicates that in both substances the characteristic time for shock propagation is R_0/c, which is actually smaller for metals than for Lucite, due to their larger values of $\rho_0 c^2$. Assuming that impact-generated shock waves propagate in essentially the same manner in all metals, this correlation would suggest that the duration of material ejection may be considerably longer than, say, the time required for the shock to degenerate down to some preassigned fraction of its initial strength. Again, measurements of shock propagation within the target are needed to resolve the question.

7. METHODS OF CRATER-SIZE PREDICTION

The success of the above analysis in predicting shock propagation is quite encouraging. However, from the viewpoint of spacecraft design, it does not solve the problem at hand, namely, to predict crater size. To accomplish such a task, additional analysis is needed. It is important to understand that every theory of crater formation contains two ingredients: first, a theory for predicting the shock-wave time history, and the flow of material behind it, and second, a criterion for choosing some point in the trajectory as the crater radius. Bjork[1], for example, chooses the instant when a stationary region of zero pressure can be found, and identifies this region by the appearance of a distribution of small velocities, which are randomly oriented.* Other authors, for example Davids and Huang[12], have used different criteria, and we shall present below some considerations of still another.

Before doing so, however, we must emphasize the central importance of the crater-formation criterion. The correlation shown in Figure 8 may be taken as evidence that, so far as shock-wave propagation is concerned, no essentially new phenomena occur over the impact-speed range up to 30 km/sec. Thus, any change in the penetration law, compared to its low-speed behavior, must be accounted for largely by the criterion used in

*Such a criterion cannot be applied in conjunction with the present solution, which never predicts a stationary region. Indeed, there is no mechanism, except for the influence of external forces, or for very special shock-wave interaction patterns, by which an inviscid fluid can be permanently brought to rest. Any analytic solution would predict that the pressure and particle velocity tend asymptotically toward zero at large time, of course, but their distributions are always nonzero, continuous, and never display a random orientation.

defining the crater radius.

This paper makes no effort to settle the question of how the crater-formation criterion should be chosen. We wish only to draw attention to the fact that its choice is a crucial element in determining the penetration law.

On the other hand, we do share with some other authors the impression that the material strength must play a role in the crater-formation criterion. The establishment of a crater of fixed size implies that material has been brought to rest, and as noted above there is no mechanism for accomplishing this feat within the framework of an inviscid theory. Thus it appears that at large time, a transition must be made to a theory which accounts for the strength of the target. Indeed, the entire hydrodynamic analysis begins with the approximation that the motion of any mass element is controlled by the pressures on its surfaces, while its resistance to shear deformation can be neglected. Whenever the inviscid theory itself predicts pressures comparable to or less than the shear strength of the target, the fundamental approximations are clearly in error. Thus we ought to assign, as a boundary for application of the hydrodynamic theory, some level of pressure comparable with the target strength.

Reference 13 not only adopts such a boundary for the fluid-dynamic theory, but actually employs it as a crater-formation criterion. In that work, the crater radius is assumed to be equal to the shock radius at the instant when the pressure behind the shock has decayed to the intrinsic strength $G/2\pi$, G being the dynamic shear modulus. This criterion was used in conjunction with the similarity solution, to deduce a penetration law which displayed reasonable agreement with experiment.

Now that a more realistic description of the shock propagation is available (from the quasi-steady theory outlined above), it is of interest to investigate the penetration law derived from the same criterion. If we require that the pressure generated at the shock be equal to a strength level designated for the moment as $\mathbb{P}$, we find from Eqs. (14) and (67) that the corresponding shock speed is given by

$$\frac{\dot{R}_s}{c} = \frac{1 + \sqrt{1 + 4s\, \mathbb{P}/\rho_o c^2}}{2} \tag{72}$$

Figure 9 gives the corresponding value of the shock radius, which, by this criterion, would be taken as the radius of the crater that will ultimately develop. Thus, the crater radius also scales with R_o :

$$R_c = k R_o = k \left(\frac{\pi/6\, \rho_P d^3 V^2}{4\pi \rho_o c^2} \right)^{1/3} \tag{73}$$

where V is the impact speed and k is shown in Figure 9. It is obvious that a large amount of experimental data could be correlated by this formula, by an empirical choice of the strength level $\mathbb{P}$. In fact, by choosing $k = \left(\frac{12 \times 10^{-9} \rho_o c^2}{B} \right)^{1/3}$, (where $\rho_o c^2$ is in cgs units, and the Brinell hardness B is measured in the customary units of kilograms force per square millimeter), the penetration law recommended by Eichelberger and Gehring[6] is recovered. Figure 10 shows a typical correlation, for aluminum projectiles striking copper targets. The parameter k has been chosen by matching the data at 3.97 km/sec.

It is interesting to note that k = 4.85, which, according to Figure 6 (with s = 1.54) means that the shock was traveling at approximately 1.3 times

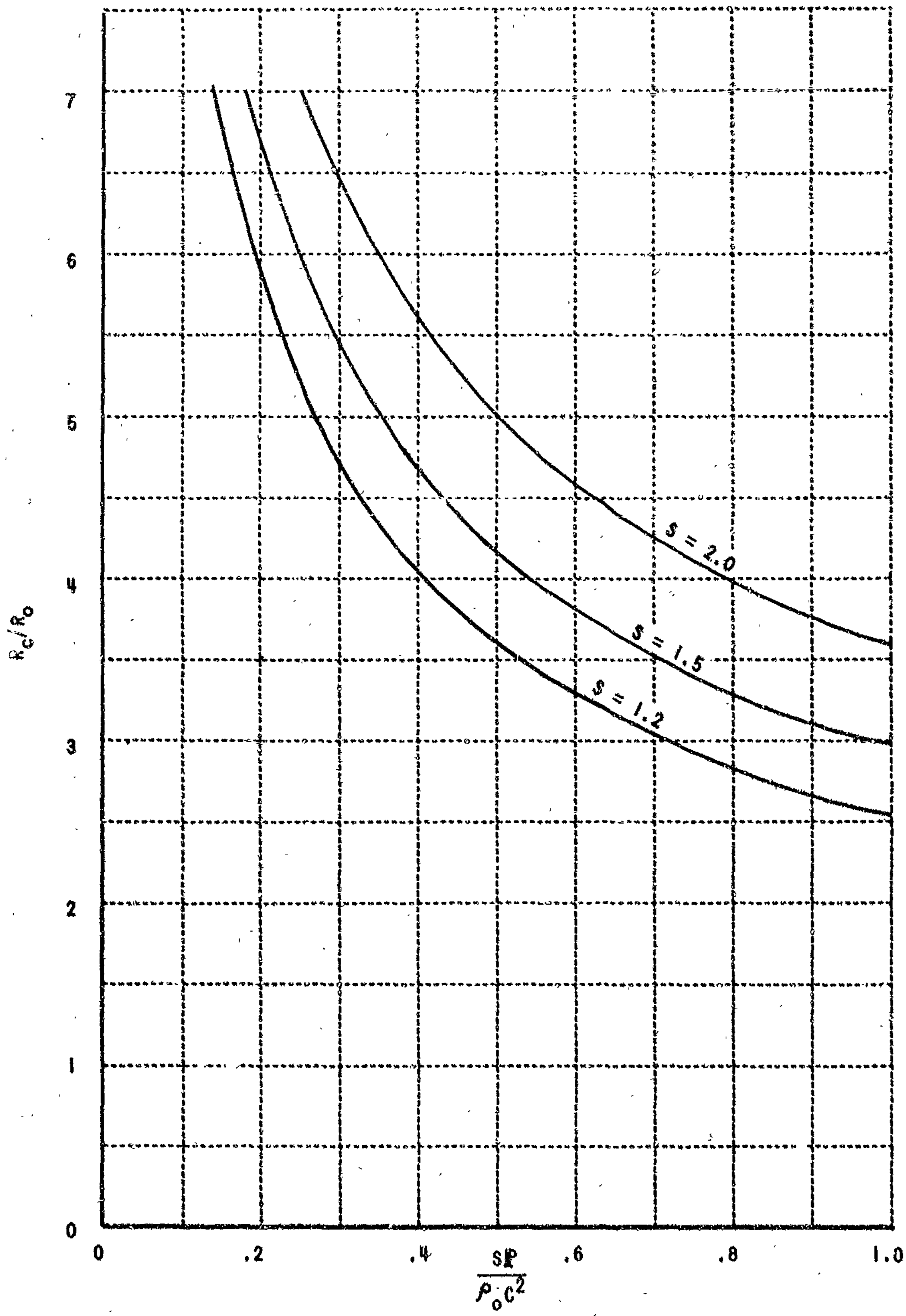

Figure 9 QUASI-STEADY PREDICTION OF SHOCK RADIUS FOR WHICH $p_1 = \mathbb{P}$

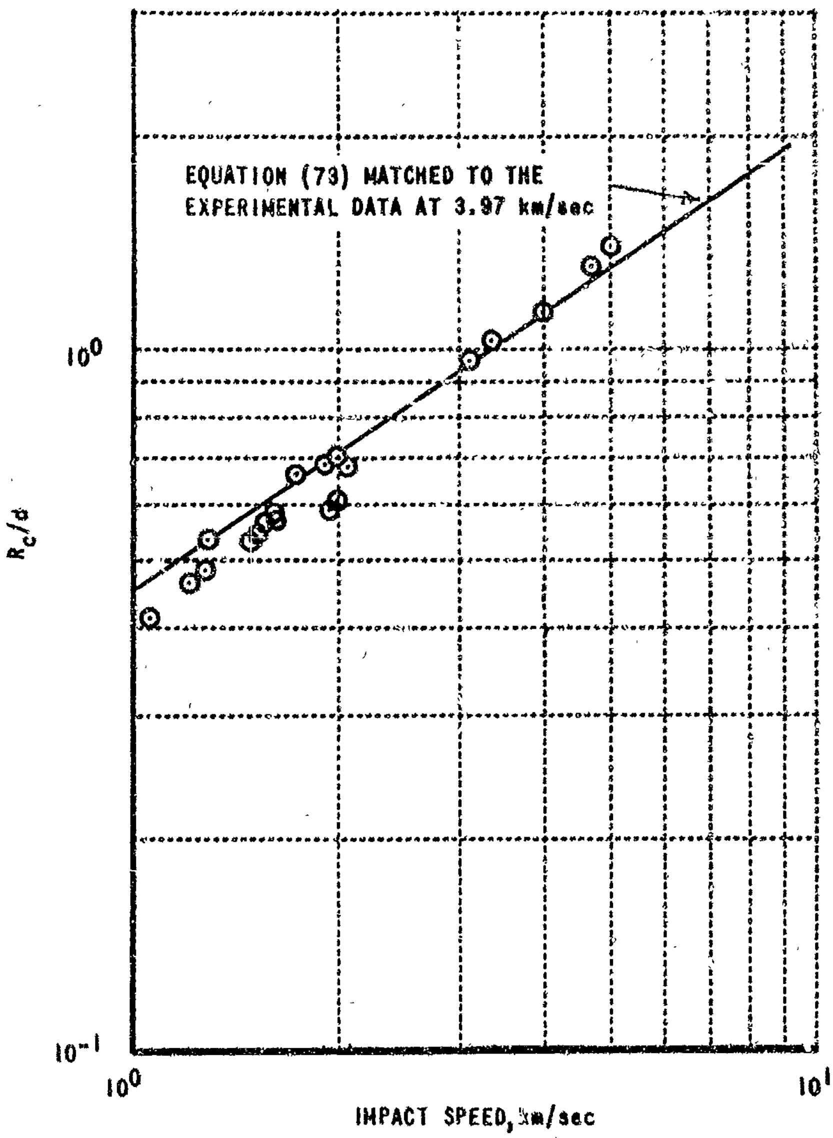

Figure 10 SEMI-EMPIRICAL CORRELATION OF CRATERS FORMED BY ALUMINUM STRIKING COPPER

the stress-wave speed when it passed the position corresponding to $\mathcal{R}_c$.

While these results are encouraging, they nevertheless contain an empirical factor whose significance is not clearly defined at present. Thus, extrapolations to higher impact speed cannot be made with confidence. Our conclusion is that there is a need for an analytical crater-formation criterion whose accuracy is comparable with that of the present quasi-steady (and of the forthcoming quasi-similar) solution. We feel that the target strength will play a role in this criterion, but that considerable work remains to be done.

CONCLUDING REMARKS

Our goal in this research has been an analytic description of hyper-velocity impact. To this end, the approximations of blast-wave theory have been reviewed to determine how well they apply to the problem of shock-wave propagation in solid targets. Most of the literature of blast-wave theory deals with the symmetric problem of a point release of energy in a gas. To adapt these analytical methods to the present problem, then, modifications are required in two areas: first, two spatial coordinates must be considered, and secondly, the equation of state appropriate to a solid must be used.

Solutions which allow for spatial variations in two directions have been found to be very close to the corresponding one-dimensional solutions in all important respects. Thus, the energy transferred by the impacting projectile is the dominant parameter, its momentum playing a minor role. Predictions of shock-wave trajectories based on this concept display excellent agreement with experiment.

The second area in which modifications of the classical blast-wave theory are needed is more significant. The nature of the state equation of solid materials, together with the fact that relatively weaker stages of shock propagation are of interest in this problem, make the assumption of similarity a weak one. Thus, shock propagation in solids is characteristically non-similar, in contrast to the situation normally encountered in gases. To account for this feature properly, analytical methods for treating nonsimilar problems must be used. Fortunately, the required methods are available, and are at present being adapted to this problem. As an interim solution, a crude approximation can be constructed from the similarity solutions themselves.

This solution, referred to here by the term "Quasi-Steady," shows remarkable agreement with the limited shock-wave trajectory data available at present. Data of this sort are the only kind that can serve as an unequivocal check on a hydrodynamical theory. Comparisons with final crater dimensions involve other aspects of the theory, especially the criterion used to define crater size, and are consequently not suitable as a check on the shock-propagation theory.

Ultimately, the practical goal of all research in this area is to establish the penetration law, especially in the high-speed regime which is experimentally inaccessible at the present time. From this point of view, the most important aspect of these studies has been to reveal the pivotal importance of the crater-formation criterion on thepenetration law. The currently available evidence suggests that impact-generated shock propagation is essentially the same over the speed range from 4.6 to 30 km/sec. Thus, any difference in penetration law is felt to originate from the crater-formation criterion. The present work makes no effort to establish what this criterion should be, though it is felt that it should be related to the strength of the target. As an example of such a criterion, a simple choice related to the pressure being generated at the shock is shown to provide a basis for correlating a large amount of data. These results are encouraging, but still contain an element of arbirariness, and their extension to the higher impact-speed range requires the development of a more satisfactory criterion.

BLAST-WAVE THEORY OF CRATER FORMATION

REFERENCES

1. Bjork, R. L., "Effects of a Meteoroid Impact on Steel and Aluminum in Space." Tenth International Astronautical Congress Proceedings, Vol. II, Springer Verlag (1960), pp. 505-514.

2. Bjork, R. L., "Analysis of the Formation of Meteor Crater, Arizona: A Preliminary Report." Journal of Geophysical Research 66 (1961), pp. 3379-3387.

3. Lees, L. and Kubota, T., "Inviscid Hypersonic Flow Over Blunt-Nosed Slender Bodies." Journal of the Aeronautical Sciences 24 (1957), pp. 195-202.

4. Cheng, H. K., Hall, J. G., Golian, T. C. and Hertzberg, A., "Boundary-Layer Displacement and Leading-Edge Bluntness Effects in High-Temperature Hypersonic Flow." Journal of the Aerospace Sciences 28 (1961), pp. 353-381.

5. Gibson, W. E. and Rudinger, G., "Analytical Study of the Dynamics of the Nuclear Bomb Cloud Rise." Cornell Aeronautical Laboratory Report No. AM-1342-A-2 (July 1960).

6. Eichelberger, R. J. and Gehring, J. W., "Effects of Meteoroid Impacts on Space Vehicles." American Rocket Society Journal 32 No. 10 (October 1962), pp. 1583-1591.

7. Halperson, S. M. and Hall, D. A., "Shock Studies in Transparent Plastic by High-Speed Photographic Techniques." Reports of NRL Progress (September 1961), pp. 37-39.

8. Frasier, J. T., and Karpov, B. G., "Impact Experiments on Wax." Proceedings of the Fifth Symposium on Hypervelocity Impact, Denver, October 30 - November 1, 1961, Vol. II, Part II (April 1962), pp. 371-388.

9. Frasier, J. T., "Hypervelocity Impact Studies in Wax." Ballistic Research Laboratories, Report No. 1124 (February 1961).

10. Sedov, L. I., "Similarity and Dimensional Methods in Mechanics." Academic Press (1959).

11. Rice, M. H., McQueen, R. G. and Walsh, J. M., "Compression of Solids by Strong Shock Waves." Solid State Physics, Advances in Research and Applications, Vol. 6, Academic Press (1958).

12. Davids, N. and Huang, Y. K., "Shock Waves in Solid Craters." Journal of the Aerospace Sciences 29 (1962), pp. 550-557.

13. Rae, W. J. and Kirchner, H. P., "Final Report on a Study of Meteoroid Impact Phenomena." Cornell Aeronautical Laboratory Report No. RM-1655-M-4 (February 1963).

14. Taylor, G. I., "The Formation of a Blast Wave by Very Intense Explosion, I, Theoretical Discussion." Proceedings of the Royal Society (A) 201 (1950), pp. 159-174.

15. Taylor, J. L., "An Exact Solution of the Spherical Blast-Wave Problem." Phil. Mag. 46 (1955), pp. 317-320.

16. Latter, R., "Similarity Solution for a Spherical Shock Wave." Journal of Applied Physics 26 (1955), pp. 954-960.

17. Sakurai, A., "On Exact Solution of the Blast-Wave Problem." J. Phys. Soc. Japan 10 (1955), pp. 827-828.

18. Davids, N., Huang, Y. K. and Jaunzemis, W., "Some Theoretical Models of Hypervelocity Impact." Proceedings of the Fifth Symposium on Hypervelocity Impact, Denver, October 31 - November 1, 1961, Vol. I, Part I (April 1962), pp. 111-132.

19. Kineke, J. H., "Observations of Crater Formation in Ductile Materials." Proceedings of the Fifth Symposium on Hypervelocity Impact, Denver, October 30 - November 1, 1961, Vol. I, Part 2 (April 1962), pp. 339-370.

20. Sakurai, A., "On the Propagation and Structure of the Blast Wave, I." J. Phys. Soc. Japan 8 (1953), pp. 662-669.

21. Oshima, K., "Blast Waves Produced by Exploding Wire." Aeronautical Research Institute, Univ. of Tokyo, Report No. 358 (July 1960).

22. Lewis, C. H., "Plane, Cylindrical, and Spherical Blast Waves Based upon Oshima's Quasi-Similarity Model." AEDC TN 61-157 (December 1961).

23. Altshuler, L. V., Bakanova, A. A. and Trunin, R. F., "Shock Adiabats and Zero Isotherms of Seven Metals at High Pressures." Soviet Physics, JETP 15 No. 1 (July 1962), pp. 65-74.

24. Franken, P., "High Energy Lasers." International Science and Technology (October 1962), pp. 62-68.

BLAST-WAVE THEORY OF CRATER FORMATION

APPENDIX

SIMULATION OF METEOROID IMPACT BY ENERGY RELEASE*

A major conclusion reached above is that crater formation is controlled chiefly by the energy of the impacting particle, its momentum playing only a secondary role. Thus we may expect to simulate hypervelocity impact by any experiment in which a strong shock wave is driven into a target by the deposition of energy in any form.

It is of central importance in considering any simulation of this type, to be certain that the mode of energy absorption does in fact drive a strong shock wave into the target. We shall return to this question below, but for the moment we assume that this condition has been achieved, and present the results that follow as a consequence.

The severity of a high-speed particle impact may be judged by the strength of the shock wave driven into the target. Knowing the Hugoniot data for the target and projectile, it is possible to solve for the shock strength as a function of the impact speed. For the case of energy deposition by some other means, we must now identify the parameters which determine the initial shock strength. The quantity that does this is the power being absorbed by the target, per unit area in the plane of the shock. To see why this is so, consider a plane shock wave of unit area advancing at speed u_s into a medium of undisturbed density ρ_0 :

*The fact that such a simulation is possible was first pointed out to the authors by Dr. Franklin K. Moore.

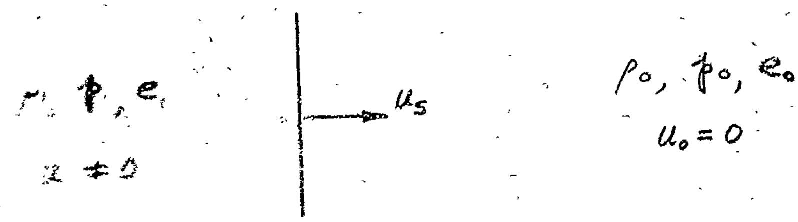

In unit time, this shock overtakes an amount of mass given by $\rho_0 u_s \, dt$, per unit area, and raises it to the energy (per unit mass)

$$e_1 = \frac{p_1}{2\rho_0}\left(1 - \rho_0/\rho_1\right)$$

Thus the rate of energy acquisition by the material behind the shock, per unit time and area, is

$$\text{power/area} = \rho_0 u_s \frac{p_1}{2\rho_0}\left(1 - \rho_0/\rho_1\right) = \frac{1}{2} p_1 u_1$$

The strength of any shock wave may therefore be characterized by the amount of power per unit area which it delivers to the medium through which it travels. The Hugoniot curve for iron is interpreted in this light in Figure 11, where it is seen that weak shock waves ($\rho_1/\rho_0 \approx 1.3$) impart about 10^{10} watts/cm^2 while extremely strong shocks ($\rho_1/\rho_0 \approx 3$) transfer to the medium some 10^{13} watts/cm^2. These orders of magnitude are typical of metals. It is interesting to note that the experiments reported by Altshuler et al[23] achieved shock waves of strength equivalent to 4×10^{11} watts/cm^2.

For a given projectile-target combination, there is a one-to-one correspondence between impact speed and the power density at the impact point. Their relation is shown in Figure 12 for iron-on-iron. The point to be noted

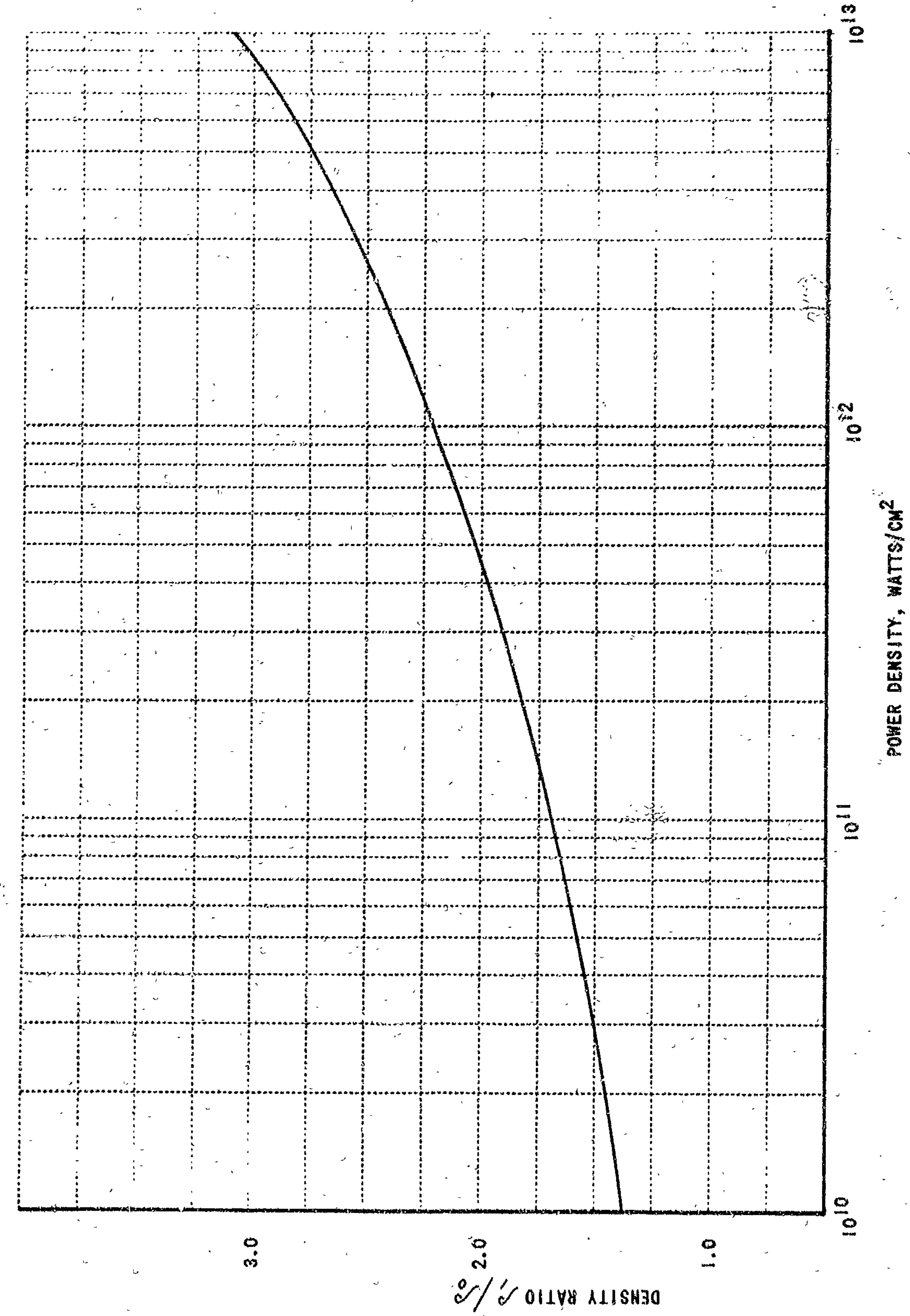

Figure 11 POWER-DENSITY RATING OF NORMAL SHOCK WAVES IN IRON

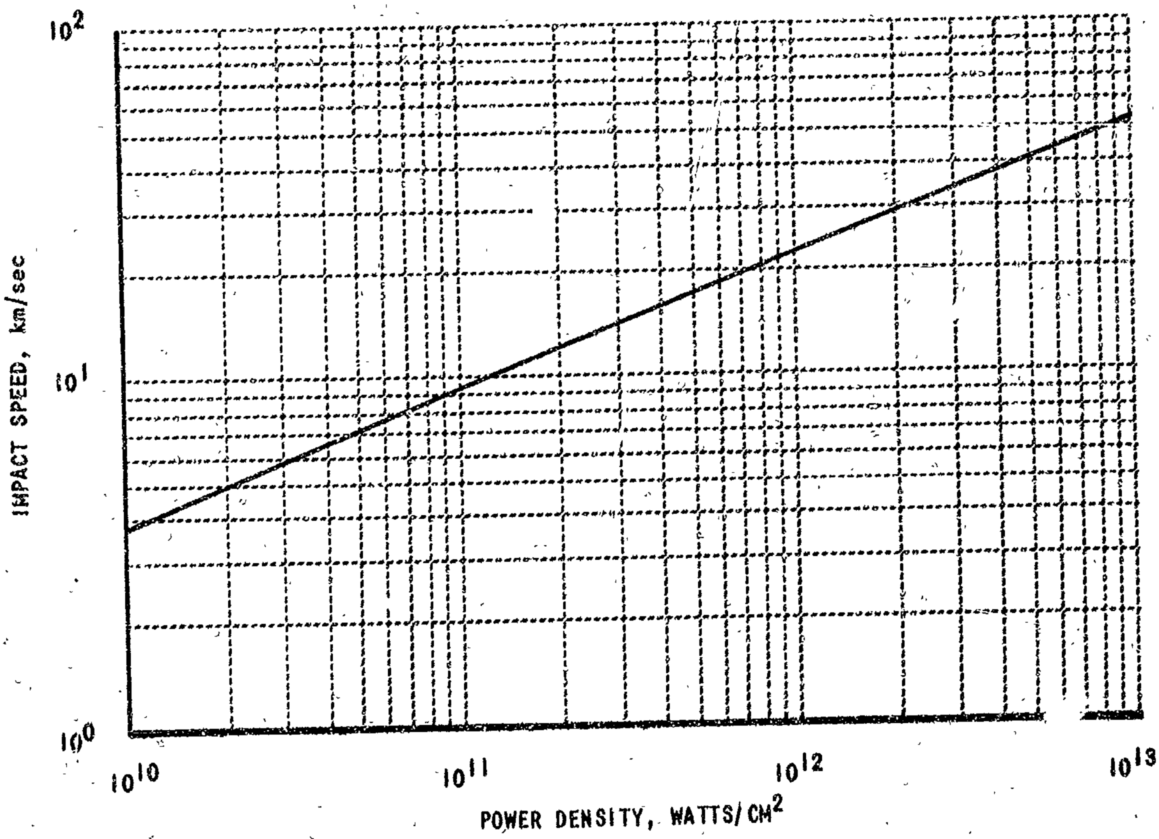

Figure 12. POWER-DENSITY RATING OF SHOCK WAVES DRIVEN INTO IRON TARGETS BY IRON PROJECTILES

is that any experimental technique capable of driving shock waves of strength greater than 10^{11} watts/cm^2 can simulate impact conditions which are at present beyond the capability of conventional projection techniques. One energy source that appears to be suitable for such an application is the laser.* By focusing the beam from such a device, power densities of 10^{13} watts/cm^2, delivered in less than a microsecond, can be delivered[24] with existing equipment. The fact that the maximum output of these devices is currently being improved at such a rapid rate indicates that, even in the presence of losses, simulation by a laser beam is a promising experimental technique.

The calculations presented in Figure 12 start from the hypothesis that the energy absorption takes place by means of a blast-wave mechanism. Particularly in the case of electromagnetic energy deposition, this assumption needs careful scrutiny. There would appear to be little doubt that this is the correct mechanism when the rate of energy input is sufficiently high. It is known that the mechanism of energy absorption in gases changes, at some point, from one of linear heat conduction to the nonlinear shock-wave mechanism. Exactly where such a transition will occur in the case of solid media is not at present known, although it is presumably amenable to theoretical analysis. The conclus ons reached above are based on the assumption that a shock wave will be the correct mechanism whenever the incident power density exceeds 10^{11} watts/cm^2.

---

*The use of such a device was suggested by Mr. A. Hertzberg.

BLAST-WAVE THEORY OF CRATER FORMATION

ACKNOWLEDGEMENT

The application of blast-wave theory to this problem was originally suggested to the authors by Dr. Franklin K. Moore. We are also indebted to Dr. Walter E. Gibson, Mr. A. Hertzberg, and Dr. Norman S. Eiss, Jr., for many valuable discussions.

Technical monitoring of this program was provided by Mr. James J. Kramer and Mr. Robert J. Denington of the Lewis Research Center. The authors are very grateful to these gentlemen for many helpful suggestions.

BLAST-WAVE THEORY OF CRATER FORMATION

LIST OF SYMBOLS

c	Velocity appearing in the relation $u_s = c + s u_1$
e	Internal energy per unit mass
E	Total energy
f	Dimensionless pressure, $p/\rho_0 \dot{R}_s^2$
g	Dimensionless internal energy $e/\dot{R}_s^2$
$I_1(\gamma)$	Integral defined by Equation (60)
N	Exponent defining rate of shock propagation: $R_s \propto t^N$
p	Pressure
P	Total momentum
$\mathbb{P}$	Strength level at which inviscid solution is terminated
R_s	Shock Radius
R_0	Length scale for shock propagation, $(E/2\pi\rho_0 c^2)^{1/3}$
r, θ	Spherical coordinates
$\mathcal{s}$	Entropy per unit mass
s	Dimensionless parameter in the relation $u_s = c + s u_1$
t	Time after impact
u, w	Velocity components in the r- and θ-directions, respectively
$\Delta(\rho)$	Function appearing in Mie-Grüneisen state equation
$\Gamma(\rho)$	Grüneisen factor
γ	Specific-heat ratio in perfect-gas model
η	Similarity coordinate, $r/R_s(t)$
ϕ	Dimensionless velocity, $u/\dot{R}_s$, positive in the direction of increasing η

$\varphi(\rho)$	Density function in state equation which allows similarity solution
ψ	Dimensionless density, ρ/ρ_0
ρ	Mass density
σ	Shear Stress
$\tau(\eta)$	$= 2\,\partial\omega/\partial\theta\,(\eta, 0)$
ω	Dimensionless velocity, $w r/\dot{R}_s$, positive in the direction of increasing θ
$(\ )_{s,\,SH}$	Evaluated at the shock
$(\ )_{0,1}$	Evaluated before, after, the shock
$(\ )_c$	Denotes cohesive contribution
$(\ )_H$	Evaluated along the Hugoniot
$(\ )'$	Ordinary derivative, $d/d\eta$